

## ORIGINAL ARTICLE

**PLATO as it is: A legacy mission for Galactic archaeology**

**A. Miglio<sup>1,2,\*</sup> | C. Chiappini<sup>3</sup> | B. Mosser<sup>4</sup> | G. R. Davies<sup>1,2</sup> | K. Freeman<sup>5</sup> | L. Girardi<sup>6</sup> | P. Jofré<sup>7,8</sup> | D. Kawata<sup>9</sup> | B. M. Rendle<sup>1,2</sup> | M. Valentini<sup>3</sup> | L. Casagrande<sup>5</sup> | W. J. Chaplin<sup>1,2</sup> | G. Gilmore<sup>7</sup> | K. Hawkins<sup>7,10</sup> | B. Holl<sup>11</sup> | T. Appourchaux<sup>12</sup> | K. Belkacem<sup>4</sup> | D. Bossini<sup>1,2</sup> | K. Brogaard<sup>1,2</sup> | M.-J. Goupil<sup>4</sup> | J. Montalbán<sup>13</sup> | A. Noels<sup>14</sup> | F. Anders<sup>3</sup> | T. Rodrigues<sup>6</sup> | G. Piotto<sup>13</sup> | D. Pollacco<sup>15</sup> | H. Rauer<sup>16,17</sup> | C. Allende Prieto<sup>18,19</sup> | P. P. Avelino<sup>20,21</sup> | C. Babusiaux<sup>22</sup> | C. Barban<sup>4</sup> | B. Barbuy<sup>23</sup> | S. Basu<sup>24</sup> | F. Baudin<sup>12</sup> | O. Benomar<sup>25</sup> | O. Bienaymé<sup>26</sup> | J. Binney<sup>27</sup> | J. Bland-Hawthorn<sup>28</sup> | A. Bressan<sup>29</sup> | C. Cacciari<sup>30</sup> | T. L. Campante<sup>31</sup> | S. Cassisi<sup>32</sup> | J. Christensen-Dalsgaard<sup>2</sup> | F. Combes<sup>33</sup> | O. Creevey<sup>34</sup> | M. S. Cunha<sup>20</sup> | R. S. de Jong<sup>3</sup> | P. de Laverny<sup>34</sup> | S. Degl'Innocenti<sup>35,36</sup> | S. Deheuvels<sup>37</sup> | É. Depagne<sup>38</sup> | J. De Ridder<sup>39</sup> | P. Di Matteo<sup>22</sup> | M. P. Di Mauro<sup>40</sup> | M.-A. Dupret<sup>14</sup> | P. Eggenberger<sup>11</sup> | Y. Elsworth<sup>1,2</sup> | B. Famaey<sup>26</sup> | S. Feltzing<sup>41</sup> | R. A. García<sup>42</sup> | O. Gerhard<sup>43</sup> | B. K. Gibson<sup>44</sup> | L. Gizon<sup>25,31,45</sup> | M. Haywood<sup>22</sup> | R. Handberg<sup>2</sup> | U. Heiter<sup>46</sup> | S. Hekker<sup>45,2</sup> | D. Huber<sup>2,47,48,49</sup> | R. Ibata<sup>26</sup> | D. Katz<sup>22</sup> | S. D. Kawaler<sup>50</sup> | H. Kjeldsen<sup>2</sup> | D. W. Kurtz<sup>51</sup> | N. Lagarde<sup>52</sup> | Y. Lebreton<sup>4,53</sup> | M. N. Lund<sup>1,2</sup> | S. R. Majewski<sup>54</sup> | P. Marigo<sup>13</sup> | M. Martig<sup>55</sup> | S. Mathur<sup>56</sup> | I. Minchev<sup>3</sup> | T. Morel<sup>14</sup> | S. Ortolani<sup>6,13</sup> | M. H. Pinsonneault<sup>57</sup> | B. Plez<sup>58</sup> | P. G. Prada Moroni<sup>35,36</sup> | D. Pricopi<sup>59</sup> | A. Recio-Blanco<sup>34</sup> | C. Reylé<sup>52</sup> | A. Robin<sup>52</sup> | I. W. Roxburgh<sup>60</sup> | M. Salaris<sup>55</sup> | B. X. Santiago<sup>61</sup> | R. Schiavon<sup>55</sup> | A. Serenelli<sup>62</sup> | S. Sharma<sup>28</sup> | V. Silva Aguirre<sup>2</sup> | C. Soubiran<sup>63</sup> | M. Steinmetz<sup>3</sup> | D. Stello<sup>2,28,64</sup> | K. G. Strassmeier<sup>3</sup> | P. Ventura<sup>65</sup> | R. Ventura<sup>66</sup> | N. A. Walton<sup>7</sup> | C. C. Worley<sup>7</sup>**

<sup>1</sup>School of Physics and Astronomy, University of Birmingham, Birmingham, UK<sup>2</sup>Stellar Astrophysics Centre, Department of Physics and Astronomy, Aarhus University, Aarhus, Denmark<sup>3</sup>Leibniz-Institut für Astrophysik Potsdam (AIP), Potsdam, Germany<sup>4</sup>LESIA, Observatoire de Paris, PSL Research University, CNRS, Université Pierre et Marie Curie, Université Paris Diderot, Meudon, France<sup>5</sup>Research School of Astronomy and Astrophysics, Mount Stromlo Observatory, The Australian National University, ACT, Australia<sup>6</sup>INAF – Osservatorio Astronomico di Padova, Padova, Italy<sup>7</sup>Institute of Astronomy, University of Cambridge, Cambridge, UK<sup>8</sup>Núcleo de Astronomía, Facultad de Ingeniería, Universidad Diego Portales, Santiago, Chile<sup>9</sup>Mullard Space Science Laboratory, University College London, Surrey, UK<sup>10</sup>Department of Astronomy, Columbia University, New York, New York<sup>11</sup>Department of Astronomy, University of Geneva, Versoix, Switzerland<sup>12</sup>Institut d'Astrophysique Spatiale, Université Paris-Sud, UMR 8617, CNRS, Orsay Cedex, France<sup>13</sup>Dipartimento di Fisica e Astronomia, Università di Padova, Padova, Italy<sup>14</sup>Space Sciences, Technologies and Astrophysics Research (STAR) Institute, Université de Liège, Liège, Belgium

-----  
 This is an open access article under the terms of the Creative Commons Attribution License, which permits use, distribution and reproduction in any medium, provided the original work is properly cited.

© 2017 The Authors. *Astronomische Nachrichten* published by WILEY-VCH Verlag GmbH & Co. KGaA, Weinheim.

- <sup>15</sup>Department of Physics, University of Warwick, Coventry, UK  
<sup>16</sup>Institute of Planetary Research, German Aerospace Center (DLR), Berlin, Germany  
<sup>17</sup>Center for Astronomy and Astrophysics, TU Berlin, Berlin, Germany  
<sup>18</sup>Instituto de Astrofísica de Canarias, La Laguna, Spain  
<sup>19</sup>Departamento de Astrofísica, Universidad de La Laguna, La Laguna, Spain  
<sup>20</sup>Instituto de Astrofísica e Ciências do Espaço, Universidade do Porto, CAUP, Porto, Portugal  
<sup>21</sup>Departamento de Física e Astronomia, Faculdade de Ciências, Universidade do Porto, Porto, Portugal  
<sup>22</sup>GEPI, Observatoire de Paris, PSL Research University, CNRS, Meudon, France  
<sup>23</sup>Departamento Astronomia, Instituto Astronômico e Geofísico, Universidade de São Paulo, São Paulo, Brazil  
<sup>24</sup>Department of Astronomy, Yale University, New Haven, Connecticut  
<sup>25</sup>Center for Space Science, NYUAD Institute, New York University Abu Dhabi, Abu Dhabi, UAE  
<sup>26</sup>Observatoire astronomique de Strasbourg, UMR 7550, Université de Strasbourg, CNRS, Strasbourg, France  
<sup>27</sup>Rudolf Peierls Centre for Theoretical Physics, University of Oxford, Oxford, UK  
<sup>28</sup>Sydney Institute of Astronomy, School of Physics, University of Sydney, NSW, Australia  
<sup>29</sup>Scuola Internazionale Superiore di Studi Avanzati, Trieste, Italy  
<sup>30</sup>INAF – Osservatorio Astronomico di Bologna, Bologna, Italy  
<sup>31</sup>Institut für Astrophysik, Georg-August-Universität Göttingen, Göttingen, Germany  
<sup>32</sup>INAF – Astronomical Observatory Teramo, Teramo, Italy  
<sup>33</sup>LERMA, Observatoire de Paris, and College de France, CNRS, PSL Univ., UPMC, Sorbonne Univ., Paris, France  
<sup>34</sup>Université Côte d’Azur, Observatoire de la Côte d’Azur, CNRS, Laboratoire Lagrange, Bd de l’Observatoire, Nice cedex 4, France  
<sup>35</sup>Dipartimento di Fisica “Enrico Fermi”, Università di Pisa, Pisa, Italy  
<sup>36</sup>INFN, Sezione di Pisa, Pisa, Italy  
<sup>37</sup>Université de Toulouse, UPS-OMP, IRAP, Toulouse, CNRS; IRAP, Toulouse, France  
<sup>38</sup>Southern African Large Telescope/South African Astronomical Observatory, Cape Town, South Africa  
<sup>39</sup>Instituut voor Sterrenkunde, KU Leuven, Leuven, Belgium  
<sup>40</sup>INAF-IAPS Istituto di Astrofisica e Planetologia Spaziali, Roma, Italy  
<sup>41</sup>Department of Astronomy and Theoretical Physics, Lund Observatory, Lund, Sweden  
<sup>42</sup>Laboratoire AIM Paris-Saclay, CEA/DRF-CNRS-Univ. Paris Diderot – IRFU/SAP, Centre de Saclay, Gif-sur-Yvette, France  
<sup>43</sup>Max-Planck-Institut für Extraterrestrische Physik, Garching, Germany  
<sup>44</sup>E.A. Milne Centre for Astrophysics, University of Hull, Hull, UK  
<sup>45</sup>Max-Planck-Institut für Sonnensystemforschung, Göttingen, Germany  
<sup>46</sup>Observational Astrophysics, Department of Physics and Astronomy, Uppsala University, Uppsala, Sweden  
<sup>47</sup>Institute for Astronomy, University of Hawaii, Honolulu, Hawaii  
<sup>48</sup>Sydney Institute for Astronomy (SfA), School of Physics, University of Sydney, NSW, Australia  
<sup>49</sup>SETI Institute, Mountain View, California  
<sup>50</sup>Department of Physics and Astronomy, Iowa State University, Ames, Iowa  
<sup>51</sup>Jeremiah Horrocks Institute, University of Central Lancashire, Preston, UK  
<sup>52</sup>Institut UTINAM, CNRS UMR6213, Univ. Bourgogne Franche-Comté, OSU THETA Franche-Comté-Bourgogne, Observatoire de Besançon, Besançon Cedex, France  
<sup>53</sup>Institut de Physique de Rennes, Université de Rennes 1, CNRS UMR 6251, Rennes, France  
<sup>54</sup>Department of Astronomy, University of Virginia, Charlottesville, Virginia  
<sup>55</sup>Astrophysics Research Institute, Liverpool John Moores University, Liverpool, UK  
<sup>56</sup>Space Science Institute, Boulder, Colorado  
<sup>57</sup>Department of Astronomy, Ohio State University, Columbus, Ohio  
<sup>58</sup>Laboratoire Univers et Particules de Montpellier, Université de Montpellier, CNRS, Montpellier, France  
<sup>59</sup>Astronomical Institute of the Romanian Academy, Bucharest, Romania  
<sup>60</sup>Astronomy Unit, School of Physics and Astronomy, Queen Mary University of London, London, UK  
<sup>61</sup>Instituto de Física, Universidade Federal do Rio Grande do Sul, Porto Alegre, RS, Brazil  
<sup>62</sup>Institute of Space Sciences (IEEC-CSIC), Cerdanyola del Valles, Spain  
<sup>63</sup>Laboratoire d’Astrophysique de Bordeaux, Univ. Bordeaux, CNRS, Pessac, France  
<sup>64</sup>School of Physics, University of New South Wales, NSW, Australia  
<sup>65</sup>INAF – Osservatorio Astronomico di Roma, MontePorzio Catone (RM), Italy  
<sup>66</sup>INAF – Osservatorio Astrofisico di Catania, Catania, Italy

**\*Correspondence**

A. Miglio, School of Physics and Astronomy, University of Birmingham, Edgbaston, Birmingham B15 2TT, UK.  
 Email: a.miglio@bham.ac.uk

**Funding information**

International Space Science Institute (ISSI), European Commission’s Seventh Framework Programme, DFG, CH1188/2-1. COST (European Cooperation in Science and Technology), ChETEC COST Action, CA16117. The Danish National Research Foundation, DNR106. UK Science and Technology Facilities Council (STFC), PRIN INAF 2014 – CRA 1.05.01.94.05, European Union FP7 program, ERC, 320360. Australian Research Council, DP150100250; FT160100402. NASA, NNX16AI09G. FCT; UID/FIS/04434/2013; FEDER (COMPETE); IF/00894/2012; POPH/FSE (EC), CNES, DLR; NYUAD Institute, G1502. “Programme National de Physique Stellaire” (PNPS), “Programme National Cosmologie et Galaxies” (CNRS/INSU, France), CNES Fellowship, Swedish National Space Board (SNSB/Rymdstyrelsen), NASA, NNX16AJ17G. ERC Consolidator (STARKEY), 615604). Belspo (PRODEX PLATO), Australian Research Council Future Fellowship, FT1400147. ESP2015-66134-R (MINECO), VILLUM FONDEN, 10118.

Deciphering the assembly history of the Milky Way is a formidable task, which becomes possible only if one can produce high-resolution chrono-chemo-kinematical maps of the Galaxy. Data from large-scale astrometric and spectroscopic surveys will soon provide us with a well-defined view of the current chemo-kinematical structure of the Milky Way, but it will only enable a blurred view on the temporal sequence that led to the present-day Galaxy. As demonstrated by the (ongoing) exploitation of data from the pioneering photometric missions CoRoT, *Kepler*, and K2, asteroseismology provides the way forward: solar-like oscillating giants are excellent evolutionary clocks thanks to the availability of seismic constraints on their mass and to the tight age–initial mass relation they adhere to. In this paper we identify five key outstanding questions relating to the formation

and evolution of the Milky Way that will need precise and accurate ages for large samples of stars to be addressed, and we identify the requirements in terms of number of targets and the precision on the stellar properties that are needed to tackle such questions. By quantifying the asteroseismic yields expected from PLATO for red giant stars, we demonstrate that these requirements are within the capabilities of the current instrument design, provided that observations are sufficiently long to identify the evolutionary state and allow robust and precise determination of acoustic-mode frequencies. This will allow us to harvest data of sufficient quality to reach a 10% precision in age. This is a fundamental prerequisite to then reach the more ambitious goal of a similar level of accuracy, which will be possible only if we have at hand a careful appraisal of systematic uncertainties on age deriving from our limited understanding of stellar physics, a goal that conveniently falls within the main aims of PLATO's core science. We therefore strongly endorse PLATO's current design and proposed observational strategy, and conclude that PLATO, *as it is*, will be a legacy mission for Galactic archaeology.

#### KEYWORDS

Galaxy: structure – stars: abundances – stars: fundamental parameters – stars: oscillations – surveys

## 1 | WHAT THIS PAPER PROVIDES

This paper spells out outstanding questions in Galactic astronomy that will still be unresolved in 10 years' time, and explains in detail how the ESA PLATO Mission<sup>1</sup> (Rauer et al. 2014), in its current form (design specification<sup>2</sup>) will be able to address these challenges.

We specify in detail the requirements on the number of targets, estimated stellar properties (including precise ages), as well as the pointing strategy requirements needed to fulfill the Galactic archaeology goals. The breakdown of this paper is as follows:

- An introduction to Galactic archaeology is given in Section 2, while key limitations and outstanding questions in the field are identified in Section 2.1.
- The need for high-precision stellar ages and the role of asteroseismology is reviewed in Section 2.2, and the requirements on the performance of PLATO as a Galactic archaeology mission are listed in Section 3.
- The expected asteroseismic yields for PLATO (red giant stars) are discussed in Section 4, and the impact of the duration of the observational campaigns on the number of stars with detectable oscillations, and on the precision of the inferred stellar properties (in particular age), is reported in Section 4.3.
- Additional constraints on stars that allow synergies with PLATO's asteroseismic data, such as distances, extinction maps, and surface gravities (hence synergies with spectroscopic surveys), are presented in Sections 4.3.1 and 4.3.2.
- Finally, a brief summary is given in Section 5.

## 2 | INTRODUCTION

Galaxies are complex systems, with dynamical and chemical substructures, where several competing processes such as mergers, internal secular evolution, gas accretion, and gas

flows take place. Galactic archaeology of the Milky Way aims at taking advantage of the fact that for our Galaxy all these processes can potentially be disentangled thanks to the use of high-dimensionality maps obtained by combining kinematic, chemical, and age information for stars belonging to the Galactic components and substructures (e.g., Freeman & Bland-Hawthorn 2002; Matteucci 2001; Pagel 2009; Rix & Bovy 2013). That researchers on Galactic science are convinced this is the way forward has become clear by the large investments in missions such as Gaia (Gaia Collaboration et al. 2016b), as well as the comparatively large efforts devoted to large-scale ground-based photometric and spectroscopic surveys (Turon et al. 2008).

Deciphering the assembly history of our Galaxy now seems a reachable goal. The complexity of the data already in hand (for instance from combining current spectroscopic information with the Gaia-TGAS sample; e.g., see Michalik et al. 2014) makes it clear that only for our Galaxy will one be able to achieve this goal in the foreseeable future. However, it has also become evident to Galactic archaeologists that one of the main pieces of the puzzle is still missing: *precise ages for stars, covering large volumes of the Milky Way* (e.g., see Chiappini 2015; Freeman 2012, and references therein). The latter requirement implies the use of red giants as tracers because these are bright enough to be observed at large distances, thus offering the opportunity to truly map the Galaxy.

The European Space Agency (ESA) Gaia satellite will soon deliver a 6D map<sup>3</sup> of  $10^5$  stars and a 5D map<sup>4</sup> of more than one billion stars throughout our Galaxy (Cacciari et al. 2016; Gaia Collaboration et al. 2016a). Additional crucial information, both on velocities and chemical abundances, will come from several ongoing/planned spectroscopic surveys such as RAVE (Kunder et al. 2017; Steinmetz et al. 2006), SEGUE-2 (Eisenstein et al. 2011; Yanny et al. 2009), APOGEE (Majewski et al. 2015; Majewski, APOGEE Team, & APOGEE- 2016), Gaia-ESO (Gilmore et al. 2012),

<sup>1</sup><http://sci.esa.int/plato/>

<sup>2</sup>Satellite with 24 cameras and a nominal 4-year observing run, built and verified for an in-orbit lifetime of 6.5 years, as described in the *PLATO Definition Study Report*.

<sup>3</sup>The star's position plus three-dimensional velocities. These are complemented by further dimensions in chemical space.

<sup>4</sup>Position plus tangential velocity.

LAMOST (Cui et al. 2012), GALAH (De Silva et al. 2015; Martell et al. 2017), WEAVE (Dalton et al. 2014), 4MOST (de Jong et al. 2014), DESI (DESI Collaboration et al. 2016a, 2016b), and MOONS (Cirasuolo et al. 2014). However, astrometric and spectroscopic constraints alone will not enable a precise and accurate estimation of red giants' ages:<sup>5</sup> here is where PLATO will play a fundamental and unique role. With PLATO, it will finally be possible to have large samples of red giants, thus covering a large volume of the Galaxy, for which precise ages will be known.

## 2.1 | Scientific motivation

The knowledge of the age of distant stars is the key to help disentangle the multidimensional problem of Galaxy assembly. Some of the pressing questions related to the origin of the oldest Galactic components such as the halo, the thick disk, and the bulge do require an age map of the oldest stars toward several directions in the Galaxy. Breakthroughs are expected if ages are known to the 10% precision level, especially at old ages (i.e., covering the first 2–4 Gyears of the evolution of our Galaxy). Moreover, ages with a 10% precision for stars in the Galaxy will let us accurately interpret the evolution of the Milky Way in the context of the evolution of disk galaxies observed at high redshift.

Indeed, the important formation phase in high- $z$  disk galaxies appears to have been between about 12 and 8 Gyear ago: after that time, thin disk formation appears to continue relatively sedately to the present. In this early interval of about 4 Gyear, the basic structure of bulges/halo, thick and thin disks in disk galaxies as we see them now, was established, as suggested by many theoretical models (e.g., Abadi et al. 2003; Bird et al. 2013; Bournaud et al. 2009; Brook et al. 2004; Gibson et al. 2009; Guedes et al. 2013; Jones & Wyse 1983; Kawata & Chiappini 2016; Noguchi 1998; Sommer-Larsen et al. 2003; Steinmetz & Mueller 1994). This seems to be also the case in the Milky Way (Chiappini et al. 1997; Chiappini 2009; Kubryk et al. 2015; Minchev et al. 2013, 2014; Snaith et al. 2015), where current data suggest that the thick disk formation started at  $z \sim 3.5$  (12 Gyear ago) while the thin disk began to form at  $z \sim 1.5$  (8 Gyear ago) (e.g., Bensby et al. 2014; Bergemann et al. 2014; Fuhrmann 2011; Haywood et al. 2013; Robin et al. 2014). The modern aim in Galactic archaeology is to build an extensive chemo-kinematical age map of the Galaxy, and finally tackle the still open questions in the field. Some of these are as follows:

1. What is the origin of the two chemically different populations of the Galactic disk, that is the  $\alpha$ -rich<sup>6</sup> and  $\alpha$ -poor disks?<sup>7</sup> The current observational evidence suggests the  $\alpha$ -rich disk to be systematically older than the  $\alpha$ -poor disk component (Fuhrmann 2011; Martig et al. 2016; Ness et al. 2016). Is there a smooth transition from an  $\alpha$ -rich to an  $\alpha$ -poor disk (Bovy et al. 2012)? Or is there a discontinuity (for instance, caused by a drop in the star formation rate) which would imply that the thick and thin disk are two genuine, discrete Galactic components with different chemical evolution histories (Chiappini et al. 1997; Reddy et al. 2006)?
2. What are the age–velocity and age–metallicity relations in the whole disk, bulge, and halo? Even for the local volume, both relations are still a matter of debate (e.g., Holmberg et al. 2007; Quillen & Garnett 2001). The radial and vertical variations of these two relations are reflected in the chemical abundance gradients in the disk (e.g., Anders et al. 2014, 2017a; Boeche et al. 2013, 2014; Cheng et al. 2012; Hayden et al. 2014; Jacobson et al. 2016; Mikolaitis et al. 2014), as well as on variations of metallicities and abundance ratios with Galactocentric distance and Galactic height (Anders et al. 2017a; Hayden et al. 2015; Rojas-Arriagada et al. 2016). All these constitute key constraints to scenarios of disk, bulge, and halo formation. Which of these Galactic components have formed inside-out, and which have formed outside-in?
3. When was the bar formed? How did the bar grow? Has the  $\alpha$ -poor disk shrunk vertically with time, or were older stars heated up by interacting with the bar, spiral arms, and/or giant molecular clouds? A map of the evolution of stellar velocity dispersions in the disk would provide important answers to questions related to the origin of the thick disk and on the main sources of heating in the disk (mergers, molecular clouds, radial migration) in chronological order. Current evolutionary models (e.g., Athanassoula et al. 2017; Di Matteo et al. 2013; Grand et al. 2016) are in desperate need for these tighter constraints.
4. Does the bulge just come from the instability of the inner thin and thick disk components, or is there a significant classical merger-generated bulge (see Bournaud 2016; Nataf 2016; Naab & Ostriker 2016; Shen & Li 2016, for recent reviews)? How is the formation of the thick disk connected to that of the bulge? Are these multi-populations responsible for the multi-peak metallicity distribution unveiled by modern data of the bulge regions (e.g., Babusiaux 2016)? What is the contribution of the inner disk to the bulge/bar (e.g., Di Matteo et al.

<sup>5</sup>Age-dating of field red giants from isochrone fitting to observations in an HR diagram is known to be a challenge, as small uncertainties on the observational constraints lead to large uncertainties on the mass (and hence age) estimates. Other recent and more indirect methods using surface abundances of carbon and nitrogen (e.g., Martig et al. 2016) are not able to deliver ages of the precision aimed for here (e.g., Lagarde et al. 2017), while spectroscopic-data-driven approaches (Casey et al. 2017; Ness et al. 2016) do require high-precision training sets to be able to deliver precise ages.

<sup>6</sup>The  $\alpha$  elements are named so because their nuclei are multiples of  $^4\text{He}$  nuclei ( $\alpha$  particles).

<sup>7</sup>These terms are often used in the literature to refer to the  $[\alpha/\text{Fe}]$  ratio, where  $[\text{X}/\text{H}] = \log(\text{X}/\text{H}) - \log(\text{X}/\text{H})_{\odot}$ . An  $\alpha$ -rich population is made of stars that have  $[\alpha/\text{Fe}] > 0.1$ – $0.2$ , depending on metallicity. This in turn is indicative of a population mainly enriched by core-collapse supernovae, and hence formed on short timescales.

2014)? What is the age distribution of the multi-peak metallicity distribution components observed in the inner regions of the Galaxy (e.g., Bensby et al. 2017)?

5. How important is radial migration? Is it so intense that it would be able to partially delete the Galactic archaeology fossil records? What is the nature and the role of the spiral arms and bar as sources of radial migration? Is migration caused by transient (Sellwood & Binney 2002) or long-lived (Minchev & Famaey 2010) patterns? How much of the radial migration is also caused by mergers (Bird et al. 2013; Quillen et al. 2009)? In relation to the disk and its merger history, how have the abundance gradients today observed in the thin and thick disks evolved? Were these gradients significantly affected by radial migration? Was the flaring of the thin disk stronger in the past (Amores et al. 2017)? As recently illustrated by Minchev et al. (2017) and references therein, ages for large samples of stars are needed to be able to tackle the above questions.

Researchers in the Galactic archaeology field are now convinced that combining asteroseismic, astrometric, and spectroscopic observational constraints provides the way forward in the field (e.g., see Noels et al. 2016, for a recent overview). Modern data will be rich in details and hence complex. The ultimate challenge will be that of building models able to interpret this rich dataset, and finally shed light on all the above questions.

## 2.2 | Why is asteroseismology needed?

One of the main challenges of Galactic archaeology in the PLATO era is to reveal the Galaxy assembly and evolution history via the age, chemical composition, and kinematics of stars in a large fraction of the volume in the Milky Way. Chemical properties and radial velocities can already be measured (at different levels of precision) by surveys such as SEGUE, RAVE, Gaia-ESO, APOGEE, LAMOST, GALAH, and, in the near future, WEAVE, 4MOST, and MOONS. The radial velocity and chemical properties for bright stars and transverse kinematics for all the stars detected by Gaia will soon be available from the upcoming Gaia data releases. These large datasets will ensure that we will have by  $\sim 2025$  a good picture of the *current* chemodynamical structure of the Milky Way. However, the critical chronological information that we need for Galactic archaeology to understand the formation and evolution of the Milky Way will still be missing.

Asteroseismology, that is the study and interpretation of and the astrophysical inference from global oscillation modes in stars, provides the way forward. Along with enabling exquisite tests of stellar models, pulsation frequencies of the solar-like oscillators may be used to place tight constraints on the fundamental stellar properties, including the radius, mass, and evolutionary state (e.g., see Chaplin & Miglio 2013, Christensen-Dalsgaard 2016, Hekker & Christensen-Dalsgaard 2016, and references therein).

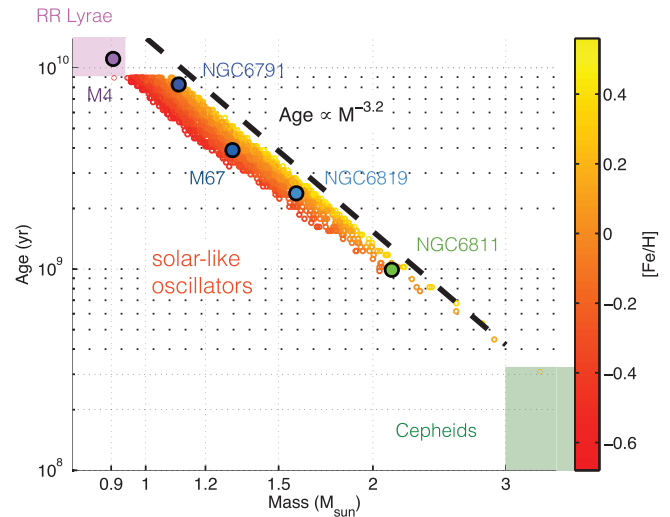


**FIGURE 1** Age–mass–metallicity relation for red giants in a TRILEGAL (Girardi et al. 2005) synthetic population representative of thin-disk red giant-branch (RGB) stars observed by *Kepler*. The dashed line indicates the average power-law relation between age and mass of RGB stars. Given their extended mass range and the tight age–mass relations, solar-like oscillating giants (dots) probe the full history of the Milky Way. The asteroseismic age scale is currently being validated primarily thanks to the detection of oscillations in giants belonging to open and globular clusters observed by *Kepler* and K2 (Arentoft et al. 2017; Brogaard et al. 2012 2016; Handberg et al. 2017; Miglio et al. 2016; Molenda-Żakowicz et al. 2014; Sandquist et al. 2016; Stello et al. 2016). Classical pulsators in similar evolutionary phases (Cepheids and RR Lyrae stars) are also indicated in the diagram

Stellar mass is a particularly valuable constraint in the case of giants, since for these stars there is a very tight relation between age and mass. The age of low-mass red giant stars is largely determined by the time spent on the main sequence, and hence by the initial mass of the red giant’s progenitor ( $\tau_{\text{MS}} \propto M/L(M) \propto M^{-(\gamma-1)}$ , with  $\gamma \sim 4$ , where  $L$  is the typical luminosity of the star on the main sequence, see e.g., Kippenhahn et al. 2012). With asteroseismic constraints on the stellar mass, it is now possible to infer the age of thousands of individual stars, spanning the entire evolution of the Milky Way (see Figure 1).

One of the most convincing (and highly regarded) statements about the importance of asteroseismology for Galactic archaeology can be found in the ESO-ESA Working groups Report 4 on Galactic populations, Chemistry and Dynamics (Turon et al. 2008). This working group was requested by ESO and ESA to consider projects that would complement the Gaia mission. One of the recommendations made to ESA was: “Asteroseismology: this is a major tool to complement Gaia with respect to age determinations. ESA should encourage the community to prepare for a next-generation mission, which would sample the different populations of the Galaxy much more widely than CNES-ESA’s CoRoT and NASA’s *Kepler*”: *PLATO is the mission that can deliver long-sought constraints to models of the Milky Way assembly and evolution.*

The combination of Gaia and spectroscopic surveys will be able to tell us the difference between photometrically

defined thick and thin disks versus chemically defined  $\alpha$ -rich and  $\alpha$ -poor disks (for a discussion regarding the various definitions of the thick and thin disks, e.g., see Kawata & Chiappini 2016; Minchev et al. 2015). Age information of turn-off stars will be available in the Gaia era. However, these stars are intrinsically faint, preventing a large volume coverage of the Galaxy (e.g., see Cacciari et al. 2016). For giants, the current age estimates are very uncertain (for instance those based on C and N spectral features, e.g., Martig et al. 2016; Masseron & Gilmore 2015) and more precise age estimates mainly rely on relatively small asteroseismic datasets from *Kepler* (Borucki et al. 2010), K2 (Howell et al. 2014), and CoRoT (Baglin et al. 2006; CoRoT Team 2016). What is needed is more reliable and homogeneously derived age information for a much larger number of stars, covering larger volumes of the Milky Way.

It has now been demonstrated that precise and more accurate (although still stellar-model-dependent) ages can be inferred for the solar-like pulsating red giants observed by the space-borne telescopes CoRoT, *Kepler*, and K2 (e.g., see Anders et al. 2017b; Casagrande et al. 2016; Miglio et al. 2013; Rodrigues et al. 2017). The combination of chemical compositions from spectroscopic surveys with distances and motions from Gaia and ages from asteroseismic data, on large samples of stars, will allow us to comprehensively study chemodynamical distributions and their time evolution in different directions of the Milky Way.

A recent application demonstrating the potential of such a combination was recently presented by Anders et al. (2017a), where around 400 stars from just two of the CoRoT fields that have measurements with APOGEE spectra (and hence velocity and chemical information) have been used to estimate the evolution of the abundance gradients in the thin disk in the last 6–8 Gyears, a long-sought constraint to the chemical evolution of the Milky Way. A further example is given by the discovery of the so-called young- $\alpha$ -rich stars (Chiappini et al. 2015; Martig et al. 2015), that is stars with masses implying young ages but which feature an overabundance in  $\alpha$ -elements, typical of old stars. It is still unclear whether the large number of young- $\alpha$ -rich stars found so far is compatible with the assumption of them being just blue stragglers rather than genuine young stars (Fuhrmann et al. 2017; Jofré et al. 2016). In addition, it will finally be possible to map the thick and thin disk components also with respect to their age, which can turn out to be the key, as the overlap in metallicities and kinematics blur our understanding of the two components. The precise measurement of the existence or not of an age gradient in the thick disk can also put strong constraints to its assembly (e.g., Minchev et al. 2015).

All of these crucial constraints will allow us to quantify the importance of stellar radial migration in the formation of the Milky Way, which is otherwise difficult to quantify from first principles. This will represent invaluable information not only for the formation of the Milky Way but also for the formation of spiral galaxies in general.

## 2.3 | What can PLATO do for Galactic archaeology that previous missions could not?

While pioneering photometric space missions such as CoRoT, *Kepler*, and K2 have demonstrated the enormous potential of seismology for stellar populations studies, they all have limitations relating to spatial and temporal coverage. *Kepler* provided a unique survey in a 105 deg<sup>2</sup> area, continuously observed during 4 years. This survey, however, provides a limited census of the Milky Way's properties.

The K2 and TESS<sup>8</sup> (Ricker et al. 2015) missions provide or will provide, respectively, a large-area and a whole-sky survey. Their results for studying the Milky Way's properties are limited by a short observation duration; the resulting frequency resolution limits the seismic analysis of evolved stars in numerous cases compared to what can be achieved by PLATO (see Section 4). The results provided by CoRoT were based on a good compromise between the extent of the survey and the observation duration, but were limited by the photon noise resulting from its 28-cm-diameter mirror and the limited sky coverage.

*PLATO is the only planned mission that can overcome these limitations*, and therefore will have an enormous impact in the field of Galactic archaeology in several ways:

1. It will provide constraints on the properties of large ensembles of stars (in the giant phase, but crucially also on the main-sequence and subgiant phase), enabling stringent tests of stellar structure and evolution models, leading to an improved accuracy on predicted stellar parameters and yields;
2. It will explore connections between populations of exoplanets and those of the host stars;
3. It will allow us to address important open questions in Galactic archaeology and will deliver the first chrono-chemo-kinematical map of the Milky Way.

In the following section we outline the specific asteroseismic performance requirements (e.g., number of stars, their spatial distribution, precision on age) needed to address the outstanding questions in Galactic archaeology. We then explore in detail (Section 4) what PLATO is expected to achieve in terms of seismic yields for red giant stars, including estimates on the precision on inferred stellar properties depending on the duration of the observational campaigns.

## 3 | PERFORMANCE REQUIREMENTS FOR A PLATO-GALACTIC ARCHAEOLOGY MISSION

The distance range to be covered by oscillating red giant stars and the need for precise ages for these objects set the

<sup>8</sup>See, e.g., Campante et al. (2016) for predictions of the asteroseismic yields of TESS.

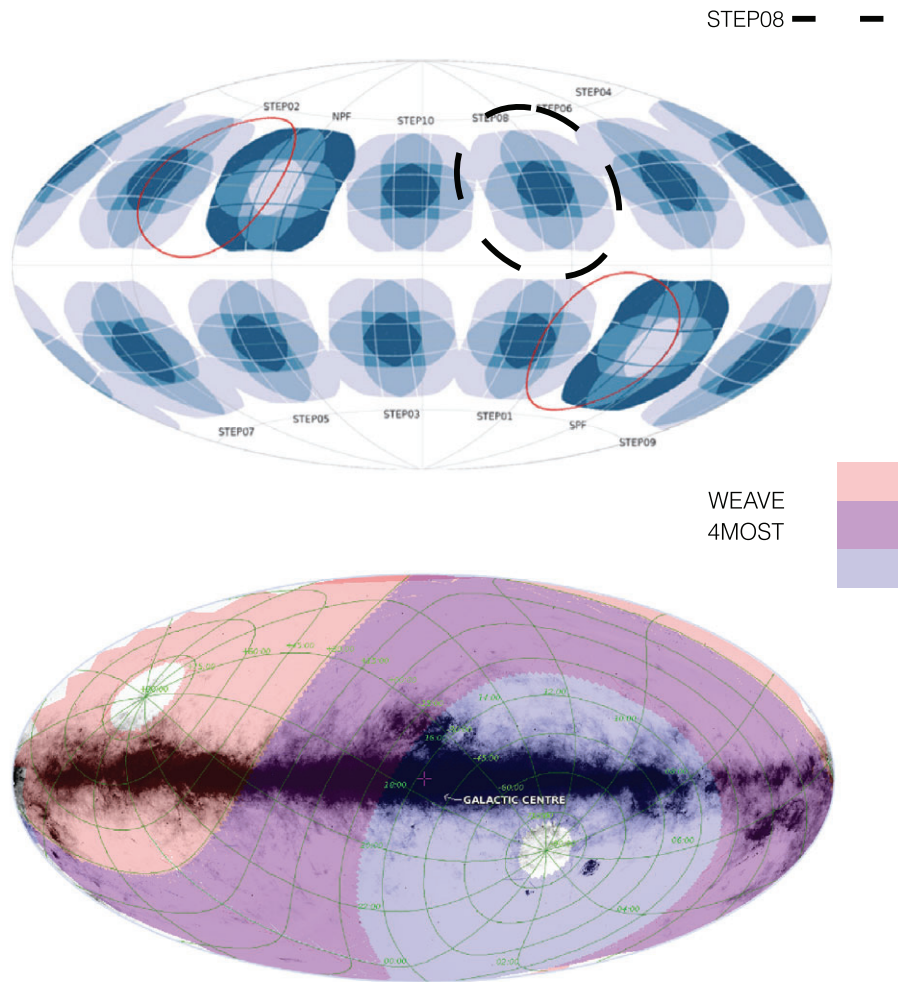


**FIGURE 2** (Upper panel) Projection of the two preliminary long-duration (LD) fields (Southern Plato Field, Northern Plato Field) and 10 step-and-stare fields (STEP01 to STEP10), all centered at  $|b| = 30$ , in the Galactic reference frame. The red line is the LD pointing requirement limit. The LD fields are color-coded on an inverted scale. In the current instrument design, various parts of each field are monitored by 24, 18, 12, or 6 cameras (as indicated by different colors). The field selected for this study (STEP08) is encircled by a thick dashed line (figure taken and adapted from the PLATO Definition Study Report). (Lower panel) Expected sky coverage of the forthcoming spectroscopic surveys 4MOST and WEAVE superposed on an IRAS map of the sky (Miville-Deschênes & Lagache 2005)

basic requirements on the limiting magnitude, the duration of observations, and the level of seismic analysis (both data analysis and modeling) required for Galactic archaeology in the PLATO era.

To ensure that the PLATO mission exploits its full legacy value also for the field of Galactic archaeology, two main requirements need to be met: (a) the observing runs need to be long enough to provide age uncertainties below  $\sim 10\%$  at the oldest ages (see Section 4), and (b) a strategic field placement is needed, enabling mapping of both the azimuthal and vertical structures of the Galactic components. The current PLATO proposal of long and short runs, as well as the planned field placement (see Figure 2), fulfills these two Galactic archaeology requirements for the following reasons:

- *Radial and vertical variations of chemo-kinematic properties of the thick and thin disks:* From current spectroscopic survey data, we know already that the properties of the

(chemically defined) Galactic thin and thick disk change with the radius and height. These changes are critical indicators of how the thin and thick disks were assembled at high redshift and subsequently evolved. To cover a useful range in radius, we need to study stars out to at least 5 kpc from the Sun. For red clump giants, and negligible extinction, this corresponds to magnitudes of about  $m_V = 14$ . Results discussed in Section 4.2.1 and Figure 3 show that this criterion is easily met and surpassed given the current mission design.

- *Radial and azimuthal variations of chemo-kinematic properties of bulge and inner disk:* Given that PLATO will be able to detect oscillations in red giant stars down to magnitudes of at least  $m_V \sim 15$ , as shown by our simulations in Section 4.2.1 and Figure 3, one should consider fields within the Galactic bulge/bar in order to establish more accurately the bulge history and its relation to the inner disk. Furthermore, given the radial and likely azimuthal dependence of chemo-kinematic properties due to the

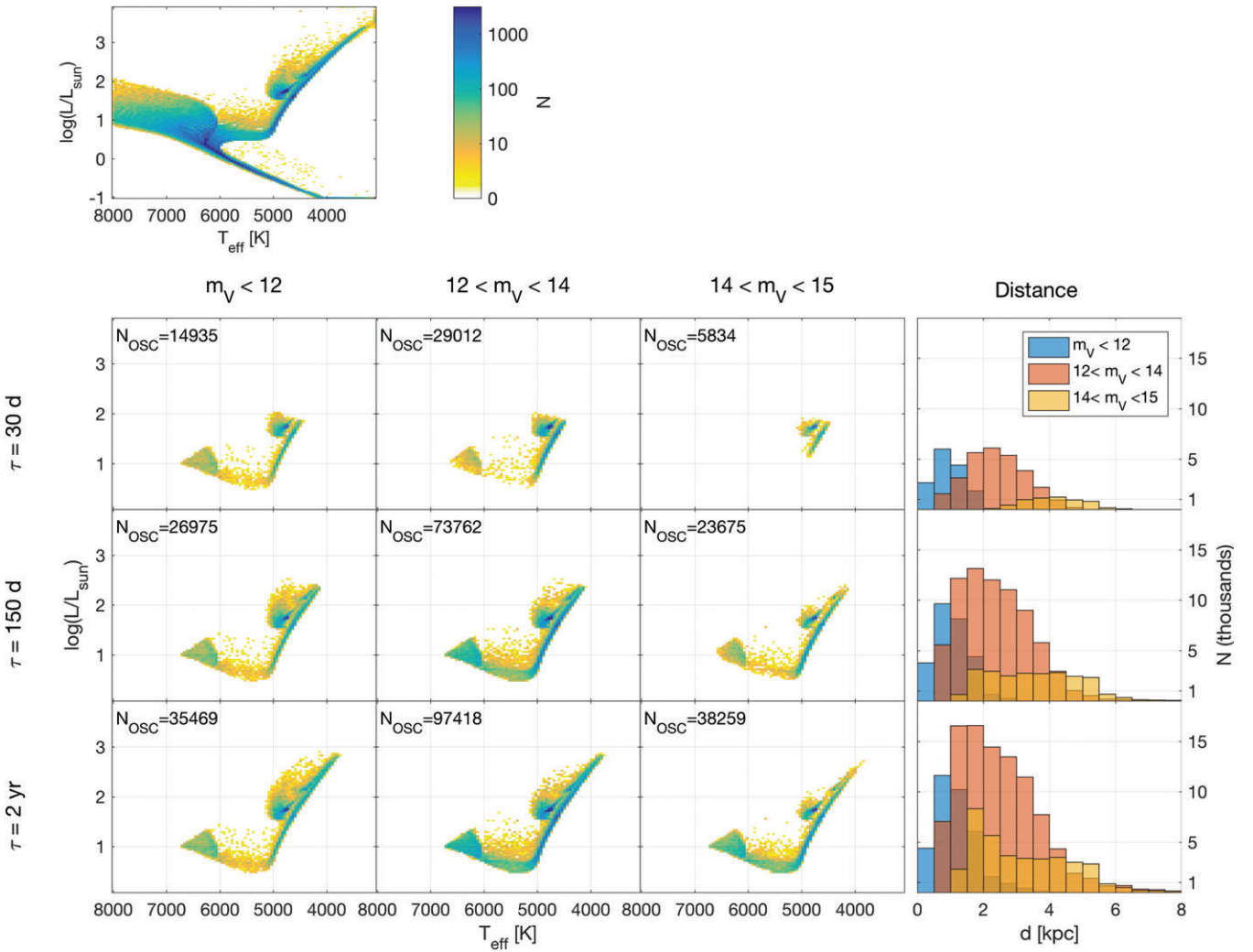


**FIGURE 3** (Upper panel) HR diagram of the synthetic population simulated with TRILEGAL in the PLATO field STEP08. Color represents the number of stars per  $T_{\text{eff}} - \log L$  bin. (Lower panel) In each row we show the HR diagram of stars with detectable oscillations and in different magnitude bins, with  $N_{\text{OSC}}$  indicating the approximate number of stars with detectable solar-like oscillations. Our predictions are limited to stars with oscillation frequencies lower than  $\sim 800 \mu\text{Hz}$ , hence primarily to stars in the red giant phase of evolution; see the main text for details. The distance distribution of such stars is presented in the right-most panel. Different rows illustrate the effect of increasing the duration of the observing run,  $\tau = 30$  days, 150 days, and 2 years (first, second, and third row, respectively)

presence of the bar and spiral arms, it is highly desirable to acquire data for giants in several Galactic fields<sup>9</sup> covering different Galactic longitudinal directions. It will be valuable to have, for instance, (a) two inner fields near Galactic longitude  $l = \pm 20$  deg and  $|b| = 30$  deg, respectively, thus sampling the inner-disk and bulge regions, and (b) another two fields at  $l = 90$  or  $270$  deg and  $l = 180$  deg ( $|b| \sim 30$  deg) to sample the whole disk well. Because the field diameter is  $\sim 45$  deg wide, at  $|b| = 30$  deg one will still reach objects close to the non-heavily-extinct Galactic plane (sampling  $|b|$  down to 10–15 deg). By adding extra fields covering even lower latitudes ( $b = \pm 4$  deg), one would be able to better explore the bulge structure (the long bar at  $l = +15$ –20 deg at  $b = 4$ –5 deg – (Wegg et al. 2015), as well as the Baade’s window at  $b = -4$  deg).

- *Mono-age populations:* The fast evolution anticipated for the earliest phases of our Galaxy (building the halo, bulge, thick disk, and the inner thin disk early on, 1–4 Gyear after the Big Bang) defines the accuracy of the ages that would be desirable for studying Galactic archaeology in this early epoch. An age precision of 10% is required to follow in detail the formation and early evolution of the thin and thick disks of our Galaxy, and in particular to identify the transition between  $\alpha$ -rich and  $\alpha$ -poor disks over large Galactic volumes (ideally  $0 < R_{\text{gal}} < 20$  kpc, and  $0 < |z| < 3$  kpc). This requirement is met and surpassed for a duration of the observation of the order of 5 months or more, as will be shown in the next sections.
- *The age-velocity dispersion relation:* In addition, with accurate age information (with uncertainties below  $\sim 1$  Gyear for the oldest age bins) for  $\alpha$ -rich and  $\alpha$ -poor

<sup>9</sup>The expected PLATO field of view at each pointing is 2232 deg<sup>2</sup>.



stars, and with a large volume coverage of the disk ( $3 < R_{\text{gal}} < 12 \text{ kpc}$  and  $0 < |z| < 3 \text{ kpc}$ ), it will be possible to measure the radial scale length and vertical scale height as a function of Galactocentric radius for mono-age disk populations. The current suggested fields, centered on  $b = 30$  but reaching  $b \sim 5 \text{ deg}$ , are ideal for this. In the redshift interval between  $z = 3$  ( $\sim 13 \text{ Gyear}$ ) and  $z = 1$  ( $\sim 8 \text{ Gyear}$ ), the velocity dispersion of the gas in star-forming disk galaxies decays from about  $80$  to about  $30 \text{ km s}^{-1}$  (e.g., Wisnioski et al. 2015). Maps of the age versus velocity dispersion at the different locations of the Galactic disk would enable the detection of a sudden change of the radial velocity dispersion at the oldest ages in case the same happens for our Galaxy.

With the above requirements fulfilled, PLATO will represent a legacy for Galactic archaeology, uncovering the Milky Way assembly history, which no other mission is able to accomplish in the foreseeable future. These data will enable the construction of maps of the radial and vertical metallicity gradients and of the width and skewness of the metallicity distribution function at different locations for mono-age populations of stars. This will provide strong constraints on the relevance of radial migration, which is closely related to the nature and strength of the spiral arms and bar, to the birth place of the Sun, as well as to the merger history of the Galaxy. By comparing these data with advanced chemodynamical simulations, it will be possible to reconstruct the metallicity distributions of mono-age populations and quantify the impact of radial migration along the Milky Way evolution. The inferred metallicity distribution of star-forming regions at different epochs will be compared with the metallicity distribution of high-redshift galaxies, which will soon be more accurately observed with Adaptive Optics and Integral Field Unit data with 30-m-class telescopes (e.g., current state of the art with KMOS/VLT seen in Wuyts et al. 2016).

As the PLATO input catalog will be based on Gaia data, one will have all the information needed for modeling the selection biases involved. In addition, possible biases related to the detectability of solar-like oscillations can be accounted for (e.g., see Chaplin et al. 2011).

## 4 | EXPECTED SEISMIC PERFORMANCE

We make use of the experience acquired with the analysis of *Kepler* observations to quantify the expected performance for PLATO. We focus on evolved stars, which represent ideal probes of Galactic structure, primarily thanks to their intrinsic brightness (see Section 2), and whose oscillations have low-enough frequencies to be detectable using PLATO long-cadence data. We refer to Rauer et al. (2014) for a discussion about the seismic performance expected for solar-like pulsating main-sequence stars.

### 4.1 | Simulating PLATO fields

The proposed PLATO fields span  $48.5\text{-deg}$ -wide squares on the sky. We simulate one of these fields, STEP08, centered at  $(l, b) = (315 \text{ deg}, +30 \text{ deg})$  (see Figure 2), using the TRILEGAL tool (Girardi et al. 2005, 2012). The entire field is initially split into small ( $0.8 \text{ deg}^2$ ) subareas by means of the healpix (Górski et al. 2005) method. For each subarea, the mean extinction and its dispersion are computed from Schlegel et al. (1998) extinction maps, and later distributed along the line of sight as if the extinction were caused by a diffuse exponential dust layer with a vertical scale height of  $110 \text{ pc}$ . In this way, nearby dwarfs are little affected by extinction while the distant giants in practice have the same distribution of extinction values as provided by Schlegel et al. (1998). The TRILEGAL model contains stars in the thin and thick disks, and halo, drawn from extended grids of stellar evolutionary and atmosphere models. They follow reasonable star formation histories and age–metallicity relations, and density distributions with well-accepted functional forms but with their total densities rescaled so that the star counts turn out to be compatible with the data from major photometric surveys such as SDSS and 2MASS (see Girardi et al. 2005, 2012, for details). As compared to observed stellar catalogs, TRILEGAL provides about the same star counts as a function of coordinates, magnitudes, and colors, but also additional information such as the evolutionary stage, mass, age, radius, and distance. Stellar properties can be straightforwardly translated into reasonable predictions of average or global asteroseismic parameters (e.g., see Chaplin & Miglio 2013): the average large frequency separation ( $\langle \Delta \nu \rangle$ ) and the frequency of maximum oscillations power ( $\nu_{\text{max}}$ ). The average separation scales, to very good approximation, as the square root of the mean density of the star, that is  $\langle \Delta \nu \rangle \propto \rho^{1/2}$ , while  $\nu_{\text{max}}$  has been found to scale with a combination of surface gravity and effective temperature that also describes the dependence of the cut-off frequency for acoustic waves in an isothermal atmosphere, that is  $\nu_{\text{max}} \propto g T_{\text{eff}}^{-1/2}$  (e.g., see Belkacem et al. 2013, for a recent review).

The HR diagram of the synthetic population simulated with TRILEGAL in the PLATO field STEP08 is shown in Figure 3.

### 4.2 | Predicting asteroseismic parameters and their detectability

We follow the approach described in Mosser (2017) based on the work by Mosser & Appourchaux (2009), and explore the effect of varying the duration of the observations ( $\tau$ ) and the apparent magnitude range ( $m_V$ ) on the asteroseismic yields expected from the underlying stellar population (see also Hekker et al. 2012). Specifically, we quantify for each star in the synthetic population:

- whether solar-like oscillations are detectable,

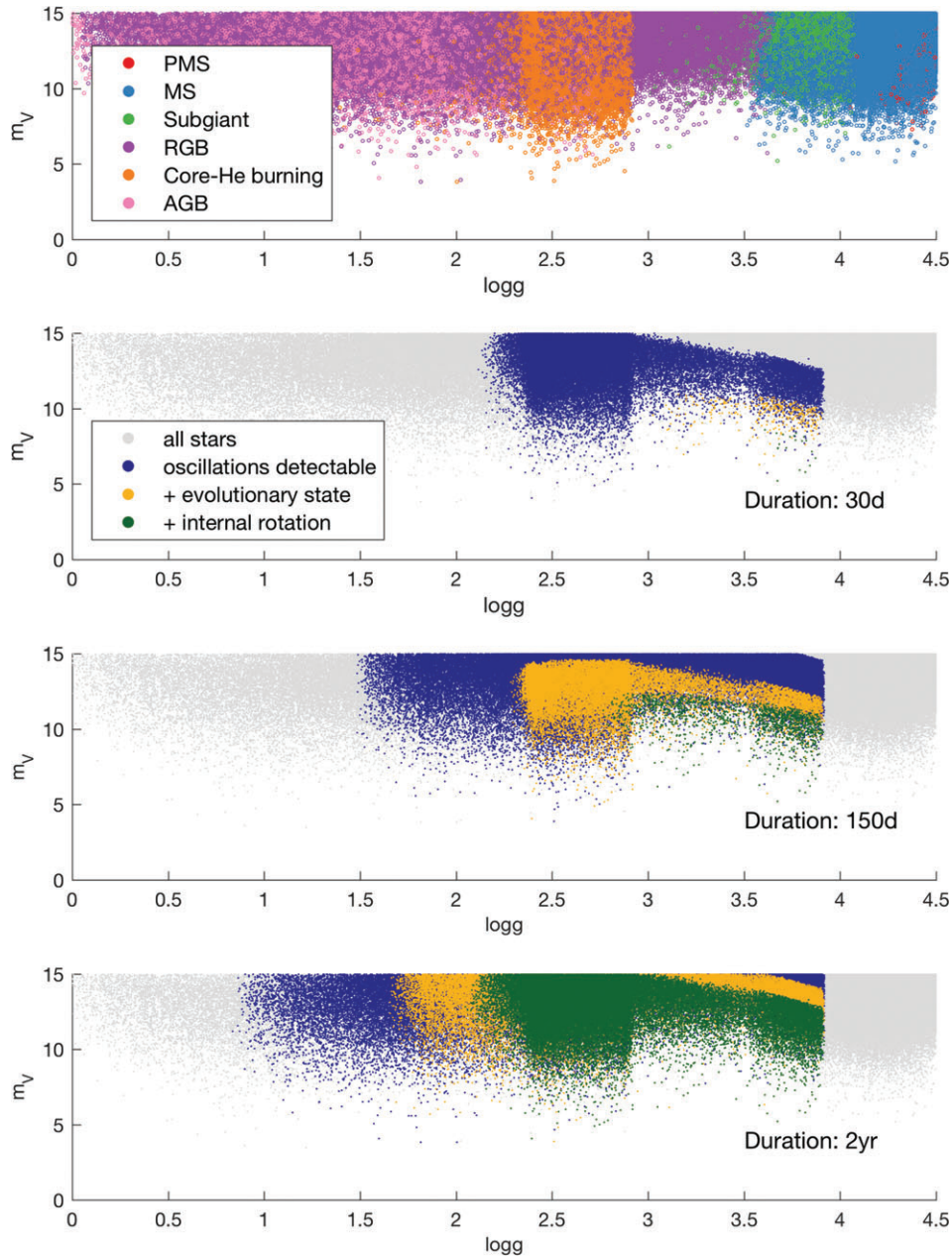


**FIGURE 4** Stars in the synthetic populations (upper panel of Figure 3) are presented in a surface gravity versus apparent V-band magnitude plot. The uppermost panel illustrates the location of stars in different evolutionary states (as defined in Bressan et al. 2012), from pre-main-sequence (PMS) to asymptotic-giant-branch (AGB) stars. The other three panels show the expected seismic yields as a function of the duration of the observations: (from top to bottom) yields for observations with durations of 30 days, 150 days, and 2 years. Each star in the population is colored according to the seismic information that can be extracted: gray, no detections; blue, oscillations are detectable (hence  $\langle \Delta \nu \rangle$  and  $v_{\max}$  can be measured); yellow, evolutionary state, based on the detection of the gravity-mode period spacing, can also be inferred; and green, rotationally split pulsation modes can be measured, hence information on the internal rotational profile can also be inferred. Our predictions are limited to stars with oscillation frequencies lower than  $\sim 800 \mu\text{Hz}$ , hence primarily to stars in their red giant phase of evolution (which are not part of PLATO’s core target list, see the main text for details)

- the expected uncertainty on  $v_{\max}$  and  $\langle \Delta \nu \rangle$ ,
- our ability to measure gravity-mode period spacing ( $\Delta P$ ), and hence to use it as a discriminant of evolutionary state (e.g., see Bedding et al. 2011),
- whether rotationally split pulsation frequencies can be measured, and hence whether information on the internal rotational profile can be inferred from the data.

Results of our simulations are presented in Figures 3, 4, and 5 and discussed in the following section.

#### 4.2.1 | Detectability of the oscillations

By increasing the duration of the observational runs, not only the overall number of stars for which oscillations are detected increases considerably (50k, 120k, 170k stars for a duration of 30 days, 150 days, and 2 years, respectively) but also larger areas of the HR diagram are covered by objects having seismic information (see Figure 3).

Moreover, the duration of the observations sets an upper limit on the radius/luminosity of stars with measurable

oscillation parameters (stars of larger radii have more closely spaced pulsation periods; for the largest stars, these periods become longer than the duration of the observations themselves). This also has implications on the distances that can be probed by such stars, for a given apparent magnitude. For instance, while the overall number of stars with detectable oscillations doubles when comparing yields from observations with durations of 150 days versus 30 days, the number of stars at distances larger than 5 kpc becomes 5 times higher (here we are considering a lower brightness limit of  $m_V = 15$ ).

The lower limit on the intrinsic luminosity of stars with detectable oscillations becomes strongly dependent on the duration of the observations, especially for stars with apparent magnitudes  $m_V > 14$  (as illustrated by Figures 3 and 4), where the detectability is hampered by the increasing noise level (and by the intrinsically low pulsational amplitudes, which decrease with decreasing luminosity—e.g., see Baudin et al. 2011; Huber et al. 2010; Kjeldsen & Bedding 1995; Samadi et al. 2012).

To account for the decreased detectability of solar-like oscillations in stars approaching the red edge of the classical pulsators instability strip, we have followed the approach described in Chaplin et al. (2011). An in-depth study of the transition between solar-like and classical pulsations, also taking into account the effects of activity on the detectability of oscillation modes (e.g., see García et al. 2010), is beyond the scope of this paper.

Another fundamental detection limit is defined by the Nyquist frequency of the time series, which in this case, assuming a cadence of 600 s, is set to 833  $\mu\text{Hz}$ ,<sup>10</sup> which is significantly higher than *Kepler*'s 278  $\mu\text{Hz}$ . This opens the door to detecting oscillations in thousands of stars during their sub-giant phase ( $\log g \simeq 3.5 - 4$ , see Figure 4). These objects are key to constraining transport processes of chemicals and the distribution (and evolution) of angular momentum inside stars (e.g., see Deheuvels et al. 2014).

As mentioned earlier, we have taken  $m_V = 15$  to be the faint magnitude limit in the simulations. However, Figure 4 suggests that, provided contamination from nearby sources is not severe, PLATO will be able to detect oscillations for fainter stars, at least if the duration of observations exceeds 30 days.

#### 4.2.2 | Seismic parameters that can be measured from the spectra

A more detailed description of what physical properties can be extracted from data of different durations can be inferred from Figure 4. We notice that a measurement of gravity-mode period spacing is most useful, for population studies at least, in stars where a possible ambiguity in the evolutionary state is

present ( $\log g \sim 2.5$ , see upper panel of Figure 4). Our simulations show that, for such stars, a precise measurement of the period spacing is possible for observations of about 5 months or longer.

Even longer datasets are required if one aims at measuring rotationally split frequencies in stars up to the core-He burning phase, which enables one to recover information about the internal rotational profile (e.g., see Beck et al. 2012; Deheuvels et al. 2012, 2014; Eggenberger et al. 2012; Mosser et al. 2012), or to infer the inclination of the star's rotational axis with respect to the line of sight (e.g., see Chaplin et al. 2013; Corsaro et al. 2017; Gizon et al. 2013; Huber et al. 2013).

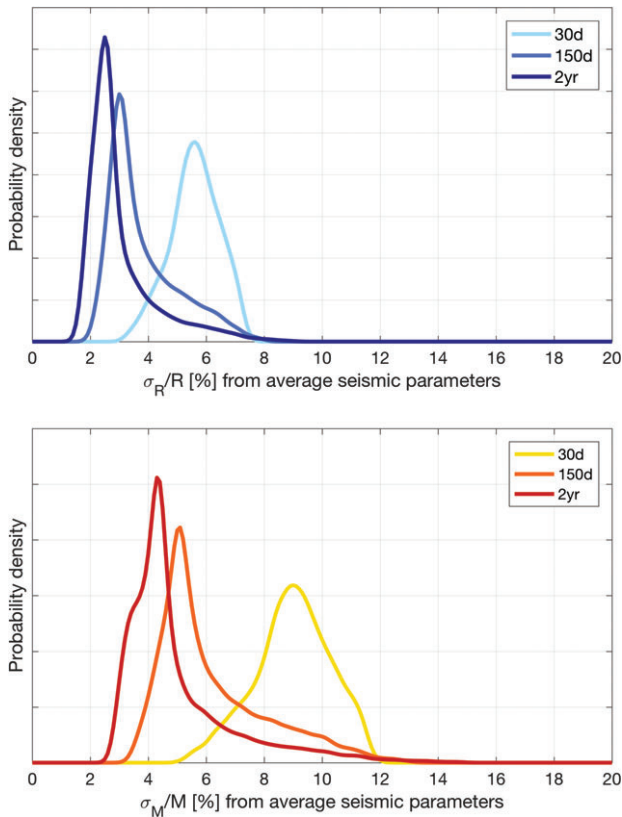
The length of the observations strongly influences both the detection yields and the precision on the measurements of the average seismic parameters of solar-like oscillators, which affects the precision of the inferred stellar properties. In our simulations we have used data on *Kepler* red giant stars to quantify the uncertainties on  $\langle \Delta\nu \rangle$  and  $\nu_{\max}$  (see Mosser 2017) for stars in the synthetic population. These uncertainties account for an irreducible limit in precision. It is about  $\langle \Delta\nu \rangle / 200$  for  $\langle \Delta\nu \rangle$  (dominated by the intrinsic variation in  $\Delta\nu$  as a function of mode frequency mainly due to acoustic glitches, e.g., see Mazumdar et al. 2012; Miglio et al. 2010; Vrad et al. 2015), and it is about  $\langle \Delta\nu \rangle / 5$  for  $\nu_{\max}$  (predominantly due to stochastic excitation and damping leading to intrinsic variability of the shape of the oscillation excess power). Estimating how the uncertainties on the measured seismic properties map onto the precision of the inferred stellar properties (primarily mass, hence age) is discussed in the next section. We notice that the uncertainties resulting from the simulations adopted here agree with the results from the approach presented in Davies & Miglio (2016), where the seismic parameters determined from varying the length of the time series representing different space missions have been compared in a case study based on a specific star.

#### 4.2.3 | Frequencies of individual pulsation modes

While average seismic parameters provide very useful estimates of global stellar properties, the highest levels of precision and accuracy are obtained when comparing observed individual frequencies to stellar models.

To assess the impact on the inferred stellar properties of the ability to measure individual mode frequencies, we have considered a typical red giant star observed by *Kepler*, with  $\nu_{\max} \sim 110 \mu\text{Hz}$ , and divided up its time series into segments of different duration. Following the approach described in Davies et al. (2016), we then determined individual-mode frequencies and their uncertainties. We have considered a star sufficiently bright so that the dominant source of background noise across the region occupied by the modes in the frequency–power spectrum is of stellar origin. As shown, for example by comparing a spectrum resulting from a 30-days-long to a 150-days-long observation (see

<sup>10</sup>This limit does not apply to low-mass main-sequence and sub-giant stars, which will be part of PLATO's core target list, and which will be studied for asteroseismology using high-cadence data (see Rauer et al. 2014).



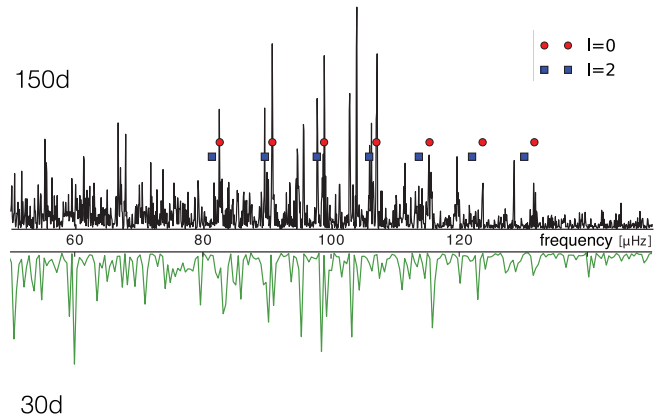
**FIGURE 5** Distribution of the expected precision on radius (upper panel) and mass (lower panel) for stars with detectable oscillations (see Figure 4). The three lines in each panel show the effect of increasing the duration of the observations, from 30 days to 2 years. Masses and radii are determined by combining  $\langle \Delta \nu \rangle$ ,  $v_{\max}$ , and  $T_{\text{eff}}$  and their uncertainties

Figure 6), a shorter length of the observations leads to a lower resolution of the power spectrum, making it harder to identify radial modes in the complex (and degraded) frequency spectrum.

We limited the analysis to radial-mode frequencies, and found that for all but the shortest time series ( $\tau = 30$  days) it was possible to determine individual-mode frequencies, albeit with complications related to disentangling radial modes from the more complex pattern of dipolar and quadrupolar modes (typically for  $\tau < 150$  days). We then focused on the 150-days-long time series, which led to uncertainties  $\sigma_v$  with values in the range  $0.04\text{--}0.09 \mu\text{Hz}$  for the seven radial modes detected, which thus have a typical relative precision of the order of  $10^{-4}\text{--}10^{-3}$ .

### 4.3 | Mapping anticipated seismic constraints onto precision of the inferred stellar properties

First, we assume that the available constraints are the average seismic parameters ( $\langle \Delta \nu \rangle$  and  $v_{\max}$ ) and  $T_{\text{eff}}$ . Examples of how the expected precision of radius and mass depends on the duration of the observations are presented in Figure 5. Although ages (and their uncertainties) cannot be inferred directly from seismic scaling relations, the uncertainty on the age is expected to be indicatively a factor of three larger than



**FIGURE 6** Power spectral density as a function of frequency obtained by considering time series of duration 150 and 30 days for a bright ( $m_V = 9$ ) giant observed by *Kepler*. The individual mode frequencies of radial ( $l = 0$ ) and quadrupolar modes ( $l = 2$ ) are indicated in the upper panel by red circles and blue squares, respectively. In the 30-days-long time series, the robust identification of individual mode frequencies is hindered by the low frequency resolution, leading to a much reduced precision and accuracy on the inferred properties of the individual modes

that on mass, based on the tight mass–age relation illustrated in Figure 1.

This means that 30-days-long observations would restrain our ability to infer ages to  $\sim 40\%$ , which is comparable to what one would expect for nearby stars without seismic constraints. On the other hand, the 150-days-long time series would lead to a twofold improvement in the precision. For a more in-depth description on how the expected uncertainties on stellar radius, mass, and age for red giant stars depend on the assumed constraints and on (some of) the uncertainties in the models, we refer to for example Noels & Bragaglia (2015), Noels et al. (2016), Casagrande et al. (2016), Rodrigues et al. (2017), and Rendle et al. (2017).

In contrast to the case of solar-like pulsating main-sequence stars (e.g., see Lebreton & Goupil 2014; Silva Aguirre et al. 2015), the effectiveness of individual mode frequencies in determining stellar properties for giant stars has yet to be fully explored. However, when individual mode frequencies are available as additional constraints, expectations are that the precision and accuracy on the inferred radii and masses (hence age) of red giants are significantly improved (Huber et al. 2013; Lillo-Box et al. 2014; Pérez Hernández et al. 2016). To illustrate the expected gain in *precision* when including radial-mode frequencies, in Figure 7 we show the posterior probability distribution functions for mass and age that we obtain by including different sets of constraints in the inference procedure. The example is limited to the 150-days-long case and shows the expected precision on a typical low-luminosity RGB star. We have assumed a length of the observations of 150 days, which would allow us to clearly identify modes, and determine the evolutionary state, and we have thus taken uncertainties on seismic parameters resulting from the simulations described above.

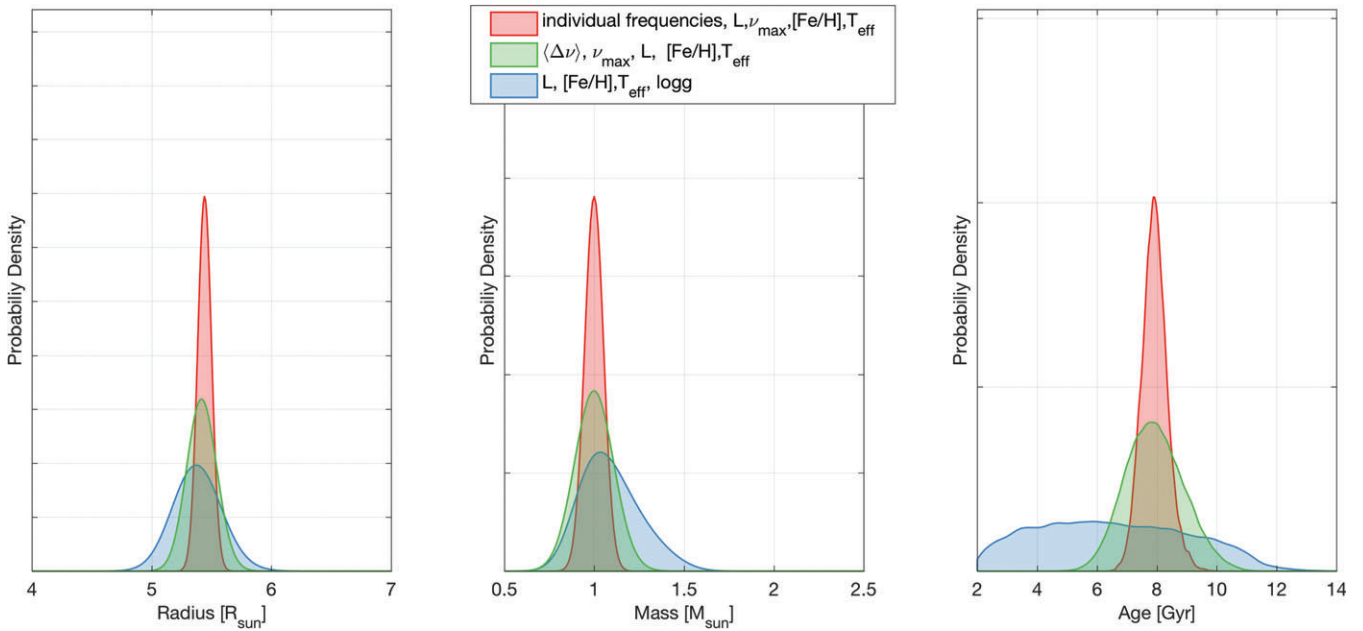


**FIGURE 7** Posterior probability density function of radius (left panel), mass (middle panel), and age (right panel) obtained by considering different combinations of seismic, spectroscopic, and astrometric constraints for a bright ( $m_V = 9$ ) RGB star with  $\nu_{\max} \sim 110 \mu\text{Hz}$ . The assumed length of the observations is 150 days. The use of individual mode frequencies is expected to provide significantly improved precision on the inferred stellar properties (see text for details)

We have then run the modeling pipeline AIMS (Reese 2016; Rendle et al. 2017) that enables statistically robust inference on stellar properties, crucially including as constraints individual mode frequencies, and compared the posterior probability distribution functions of radius, mass, and age assuming astrometric and spectroscopic constraints only ( $T_{\text{eff}}$ ,  $[\text{Fe}/\text{H}]$ ,  $\log g$ , and luminosity as expected from Gaia for a nearby star), and then adding either average seismic constraints ( $\langle \Delta\nu \rangle$ ,  $\nu_{\max}$ ) or individual radial mode frequencies. We assumed the following uncertainties on non-seismic constraints: 0.2 dex in  $\log g$ , 0.15 dex in  $[\text{Fe}/\text{H}]$ , and 3% in luminosity (see Rodrigues et al. 2017 for additional tests).

When compared to the case of spectroscopic and astrometric constraints only, one can expect a 2.5-fold improvement in the precision on age when adding average seismic constraints, and a dramatic sixfold improvement when one is able to make use of the much more precise individual radial mode frequencies. Data of such quality would thus make it possible to reach the desired precision in age ( $\lesssim 10\%$ ). For the more ambitious goal to achieve similar level of accuracy, one would have to couple these data with stringent tests of models of stellar structure and evolution, which is one of the core science aims of the PLATO mission.

#### 4.3.1 | Distances and interstellar reddening

Seismic constraints can be combined with effective temperature and apparent photometric magnitudes to determine distances (see Figure 8 and Anders et al. 2017b; Mathur et al. 2016; Miglio et al. 2013; Rodrigues et al. 2014). Such distances typically reach a level of precision of few percent (2–5%, depending on the duration of the observations, e.g.,

see Rodrigues et al. 2014). Similar to the period–luminosity relations for classical pulsators, their precision depends little on the distance itself as long as a robust detection of the oscillations is achievable. Consequently, seismic distances will have comparable if not superior precision to Gaia for stars with  $m_V \gtrsim 13$ , that is giant stars beyond  $\sim 3$  kpc (see Figure 9 and Huber et al. 2017). One could thus select targets to ensure that PLATO can also significantly improve the cartography of the Milky Way, given that oscillations are expected to be detectable for significantly fainter magnitudes (see Section 4.2.1 and Figure 4). We note also that the prime targets for PLATO, that is bright stars, will play a fundamental role in testing the accuracy of the seismic distance scale, benefiting from negligible extinction as well as exquisite seismic, spectroscopic, photometric, and astrometric data, and, for some targets, interferometric constraints (e.g., see Huber et al. 2012; Lagarde et al. 2015; Silva Aguirre et al. 2012).

Moreover, as a byproduct of the analysis, 3D reddening maps can be determined by fitting the spectral energy distributions in several photometric bands, and combining them with spectroscopic effective temperatures and precise bolometric luminosities from seismology (see Rodrigues et al. 2014, for a detailed description of the method).

#### 4.3.2 | Synergies with spectroscopic surveys

An additional stellar property that asteroseismic constraints can deliver with high precision is surface gravity ( $\sigma_{\log g} \lesssim 0.05$  dex, e.g., see Morel 2015, and references therein). Given the difficulties associated with measuring  $\log g$  via spectroscopic analyses, large-scale spectroscopic surveys have now included solar-like oscillating stars among their targets, as key

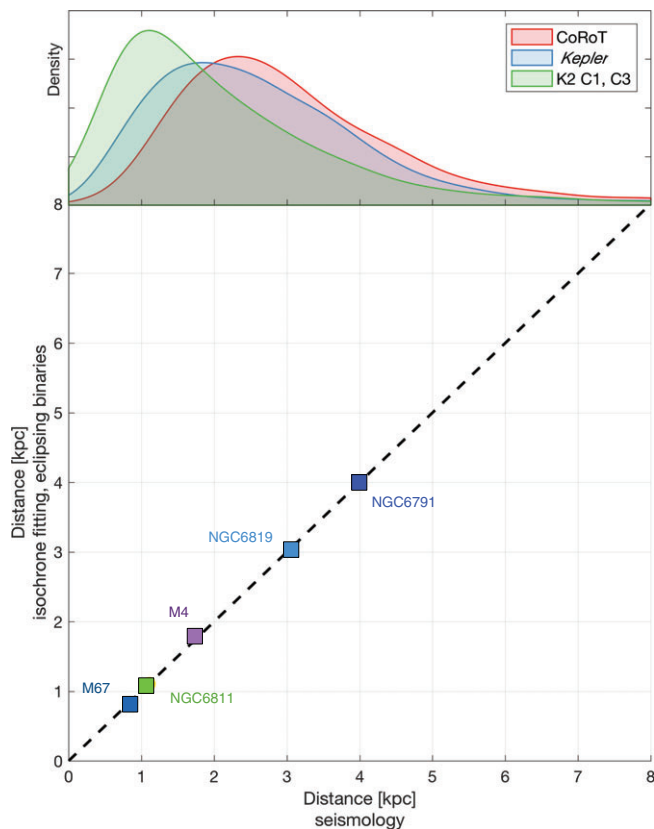


**FIGURE 8** (Lower panel) Asteroseismic distance scale for solar-like oscillating giants, presenting a comparison between seismic distances against benchmark distances of clusters, the latter obtained via isochrone fitting and/or based on eclipsing binaries. Distances are taken from Brogaard et al. (2016), Miglio et al. (2016), Stello et al. (2016), Handberg et al. (2017), Sandquist et al. (2016), and Molenda-Żakowicz et al. (2014). (Upper panel) Distribution of distances for targets in various asteroseismic missions. The different duration of the observations, coupled with the mission-specific target selection function, explains the different distributions. Longer observations allow the measurement of oscillations in longer period (hence, in general, intrinsically brighter and more distant) stars. CoRoT, in its so-called exo-field, targeted stars fainter than *Kepler*

calibrators of surface gravity. For instance, CoRoT targets are now being observed by the Gaia-ESO Survey (Valentini et al. 2016), APOGEE (Anders et al. 2017b), and GALAH (Martell et al. 2017). *Kepler* targets have been used for calibrating stellar surface gravities in APOGEE (Pinsonneault et al. 2014) and LAMOST (Wang et al. 2016).

Recently, K2 targets at different locations (e.g., see Howell et al. 2014; Stello et al. 2015) have become the key stars for cross-calibrating several surveys. An example of the impact of having seismic surface gravities for several stars included in spectroscopic surveys has been recently shown for RAVE. The RAVE survey collected intermediate-resolution spectra around the Ca triplet. This wavelength interval, despite being excellent for deriving radial velocities, contains few spectral lines resulting in degeneracies of stellar parameters: lines produced in stars with different surface gravities and at the same temperature are hardly discernible, as illustrated in Figure 10. K2 observed 87 RAVE red giants during Campaign 1, and the seismically inferred surface gravity provided a calibration for

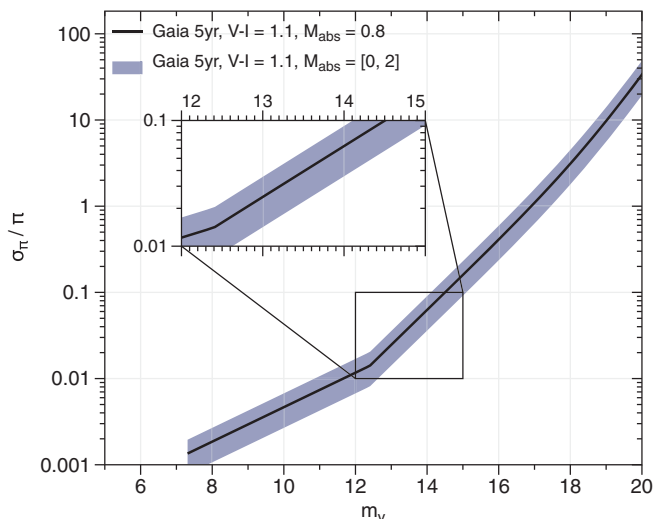


**FIGURE 9** Gaia's end-of-mission relative parallax error, evaluated for typical red giant stars with detectable solar-like oscillations. The solid line illustrates the case of stars with an absolute  $V$ -band magnitude representative of red-clump stars. The precision achieved by seismology (few percent) is comparable to or better than Gaia's for stars fainter than  $m_V = 13 - 14$  (i.e., distances  $\gtrsim 3$  kpc, see also Huber et al. 2017). Gaia parallax performance estimate adapted from <https://www.cosmos.esa.int/web/gaia/science-performance> (using astrometric error model of de Bruijne et al. 2005 and color transformation of Jordi et al. 2010)

the  $\log g$  for giants (Valentini et al. 2017). Abundances have been recomputed then using these newly *calibrated* gravities, and presented in the RAVE-DR5-SC catalog (Kunder et al. 2017).

Additionally, beyond improving stellar parameters derived from spectra, seismic information has become critical in the era of high-precision chemical abundance determination analyses. In a new approach, where atmospheric parameters are computed by *fixing*  $\log g$  to the seismic value, and iteratively deriving the surface temperature and overall metallicity  $[M/H]$  (thus ensuring high consistency among all stellar parameters), Morel et al. (2014) and Valentini et al. (2016, 2017) have demonstrated that higher accuracy on chemical abundances can be achieved.

A further example was shown using high-resolution ( $R \sim 22,500$ ) spectra from APOGEE, in the  $H$ -band ( $1.5 - 1.7 \mu\text{m}$ ). In this wavelength regime, there is a lack of usable Fe II lines, which are widely used to constrain the surface gravity spectroscopically. Building on the work of Pinsonneault et al. (2014), Hawkins et al. (2016) was able to show that using the seismic information (and adopting the APOGEE surface temperatures) one can *significantly* improve the precision and accuracy of stellar parameters and chemical abundances derived from APOGEE spectra. The seismic data for the APOGEE+*Kepler* sample has also been used to identify the spectral regions that are most sensitive to  $\log g$  which can be used to find novel ways of constraining this difficult parameter beyond the standard Fe

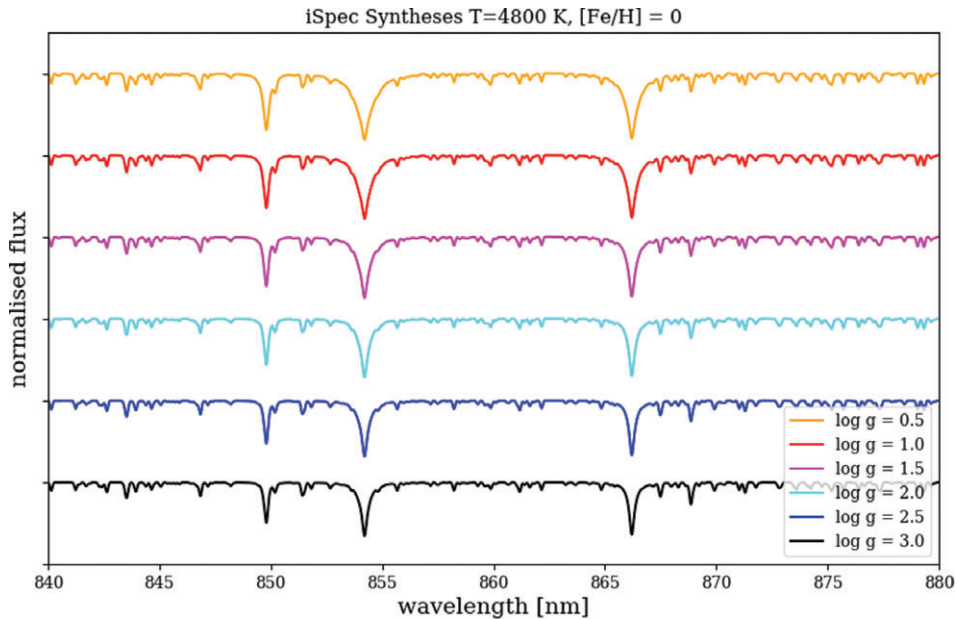


**FIGURE 10** Synthetic spectra of a solar-metallicity star with  $T_{\text{eff}} = 4800$  K in the wavelength range and resolution of RAVE. Each line represents a spectrum with different  $\log g$ , from 0.5 to 3.0 in steps of 0.5 dex, showing how little spectral features change with surface gravity. Spectra are synthesized using the iSpec package (Blanco-Cuaresma et al. 2014), considering the Turbospectrum (Plez 2012) radiative transfer code and MARCS (Gustafsson et al. 2008) atmosphere models

II ionization balance technique (e.g., Masseron & Hawkins 2017).

The spectroscopic follow-up of PLATO’s targets by several planned large-scale surveys (e.g., 4MOST, WEAVE, SDSS-V, see also Figure 2) will not only be beneficial to the calibration of spectroscopic analysis procedures but will also allow precise chemical abundance determinations that are key to inferring precise stellar properties (in particular age), to test stellar models, and, notably, for informing models of Galactic chemical evolution and to help identify populations of stars with a common origin (e.g., see Freeman & Bland-Hawthorn 2002). In particular, observing how individual star clusters have spread out is the most direct measure of radial migration with cosmic time (Bland-Hawthorn et al. 2010).

## 5 | SUMMARY

Deciphering the assembly history of the Milky Way is a formidable task, which becomes possible only if one can produce high-resolution chrono-chemo-kinematical maps of the Galaxy.

Currently, a wealth of data is being gathered on ensembles of stars with the aim of improving our knowledge of the Milky Way structure and of its chemodynamical properties. The ESA Gaia satellite, with its second data release, will soon deliver an accurate 3D map and proper motions of all detected stars, as well as radial velocities for bright stars throughout our Galaxy. Additional crucial information, both on velocities and chemical abundances, will come from several ongoing/planned spectroscopic surveys such as

RAVE, SEGUE, APOGEE, Gaia-ESO, LAMOST, GALAH, WEAVE, and 4MOST. These data will soon provide us with a well-defined view on the current chemo-kinematical structure of the Milky Way, but will only enable a blurred view on the temporal sequence that led to the present-day Galaxy. The framework for chemodynamical models tailored to the Milky Way now exists (e.g., Minchev et al. 2014), as well as tools to best compare model predictions to the data (e.g., Anders et al. 2016; Sharma et al. 2011).

Astrometric and spectroscopic constraints alone will not enable precise and accurate estimates of stellar age. This is particularly true for red giant stars, which are the primary tracers of the Milky Way’s structure. Asteroseismology clearly provides the way forward: solar-like oscillating giants are excellent clocks thanks to the availability of seismic constraints on their mass and to the tight age–initial mass relation they adhere to. The potential of asteroseismology for constraining evolutionary models of the Milky Way has now been demonstrated thanks to the ongoing exploitation of data from the pioneering photometric missions CoRoT, *Kepler*, and K2.

These missions, however, are limited in either Galactic volume coverage or duration of the observations, which limits the precision one can achieve on the inferred stellar properties, chiefly age. In this paper we have identified five key questions (see Section 2.1) that we believe will need precise and accurate ages for large samples of stars to be addressed, and identified the requirements in terms of the number of targets and the precision on the stellar properties that are needed to tackle such questions (Section 3).

By quantifying the seismic yields expected from PLATO, we have shown in Section 4 that the requirements outlined in Section 3 are within the capabilities of the current PLATO design, provided that observations are sufficiently long to identify the evolutionary state and allow robust and precise determination of acoustic-mode frequencies. This will allow us to harvest data of sufficient quality to reach a 10% precision in age. This is a fundamental prerequisite to then reach the more ambitious goal of a similar level of accuracy, which will be possible only if coupled with a careful appraisal of systematic uncertainties on age deriving from our limited understanding of stellar physics; a goal that conveniently falls within the main aims of PLATO's core science. *We therefore strongly endorse PLATO's current design and proposed observational strategy, and conclude that PLATO, as it is, will be a legacy mission for Galactic archaeology.*

## ACKNOWLEDGMENTS

We are extremely grateful to the International Space Science Institute (ISSI) for the support provided to the asterosSTEP ISSI International Team.<sup>11,12</sup> This article made use of AIMS, a software for fitting stellar pulsation data, developed in the context of the SPACEINN network, funded by the European Commission's Seventh Framework Programme. This research has made use of "Aladin sky atlas" developed at CDS, Strasbourg Observatory, France. C.C. acknowledges support from DFG Grant CH1188/2-1 and from the ChETEC COST Action (CA16117), supported by COST (European Cooperation in Science and Technology). Funding for the Stellar Astrophysics Centre is provided by The Danish National Research Foundation (Grant agreement no.: DNR106). A.M., G.R.D., W.J.C., and I.W.R. acknowledge the support of the UK Science and Technology Facilities Council (STFC). L.G. and T.S. acknowledge support from PRIN INAF 2014 – CRA 1.05.01.94.05. P.J. acknowledges European Union FP7 program through ERC grant number 320360. L.C. gratefully acknowledges support from the Australian Research Council (grants DP150100250, FT160100402). S.B. acknowledges NASA grant NNX16AI09G. M.C. and P.P.A. acknowledge support from FCT through the grant UID/FIS/04434/2013 and the contract IF/00894/2012/ and POPH/FSE (EC) by FEDER funding through the program COMPETE. R.A.G. acknowledges the support from CNES. L.Gizon acknowledges research funding from DLR under the PLATO Data Center and from the NYUAD Institute under grant no. G1502. N.L. thanks financial support from "Programme National de Physique Stellaire" (PNPS) and from "Programme National Cosmologie et Galaxies" of CNRS/INSU, France. N.L. acknowledges financial support from the CNES fellowship. U.H. acknowledges support from the Swedish National Space

Board (SNSB/Rymdstyrelsen). S.M. acknowledges support from the NASA grant NNX16AJ17G. P.M. and J.M. acknowledge support from the ERC Consolidator Grant funding scheme (*project STARKEY*, G.A. n. 615604). T.M. acknowledges financial support from Belpo for contract PRODEX PLATO. D.S. is the recipient of an Australian Research Council Future Fellowship (project number FT1400147). A.S. acknowledges funding from ESP2015-66134-R (MINECO). V.S.A. acknowledges support from VILLUM FONDEN (research grant 10118).

## REFERENCES

- Abadi, M. G., Navarro, J. F., Steinmetz, M., & Eke, V. R. 2003, *ApJ*, 591, 499.
- Amores, E. B., Robin, A. C., & Reyle, C. 2017, ArXiv e-prints.
- Anders, F., Chiappini, C., Minchev, I., et al. 2017a, *A&A*, 600, A70.
- Anders, F., Chiappini, C., Rodrigues, T. S., et al. 2017b, *A&A*, 597, A30.
- Anders, F., Chiappini, C., Rodrigues, T. S., et al. 2016, *AN*, 337, 926.
- Anders, F., Chiappini, C., Santiago, B. X., et al. 2014, *A&A*, 564, A115.
- Arentoft, T., Brogaard, K., Jessen-Hansen, J., et al. 2017, ArXiv e-prints.
- Athanassoula, E., Rodionov, S. A., & Prantzos, N. 2017, *MNRAS*, 467, L46.
- Babusiaux, C. 2016, *PASA*, 33, e026.
- Baglin, A., Auvergne, M., Barge, P., et al. 2006, in: The CoRoT Mission Pre-Launch Status — Stellar Seismology and Planet Finding, eds. M. Fridlund, A. Baglin, J. Lochard, & L. Conroy, ESA Special Publication, Vol. 1306, 33.
- Baudin, F., Barban, C., Belkacem, K., et al. 2011, *A&A*, 529, A84.
- Beck, P. G., Montalbán, J., Kallinger, T., et al. 2012, *Nature*, 481, 55.
- Bedding, T. R., Mosser, B., Huber, D., et al. 2011, *Nature*, 471, 608.
- Belkacem, K., Samadi, R., Mosser, B., Goupil, M.-J., & Ludwig, H.-G. 2013, in: Progress in Physics of the Sun and Stars: A New Era in Helio- and Asteroseismology, eds. H. Shibahashi & A. E. Lynas-Gray, ASP Conf. Ser., Vol. 479, 61.
- Bensby, T., Feltzing, S., Gould, A., et al. 2017, ArXiv e-prints.
- Bensby, T., Feltzing, S., & Oey, M. S. 2014, *A&A*, 562, A71.
- Bergemann, M., Ruchti, G. R., Serenelli, A., et al. 2014, *A&A*, 565, A89.
- Bird, J. C., Kazantzidis, S., Weinberg, D. H., et al. 2013, *ApJ*, 773, 43.
- Blanco-Cuaresma, S., Soubiran, C., Heiter, U., & Jofré, P. 2014, *A&A*, 569, A111.
- Bland-Hawthorn, J., Krumholz, M. R., & Freeman, K. 2010, *ApJ*, 713, 166.
- Boeche, C., Siebert, A., Piffl, T., et al. 2014, *A&A*, 568, A71.
- Boeche, C., Siebert, A., Piffl, T., et al. 2013, *A&A*, 559, A59.
- Borucki, W. J., Koch, D., Basri, G., et al. 2010, *Science*, 327, 977.
- Bournaud, F. 2016, Galactic Bulges Astrophysics and Space Science Library; Springer International Publishing: Switzerland. 418, 355.
- Bournaud, F., Elmegreen, B. G., & Martig, M. 2009, *ApJ*, 707, L1.
- Bovy, J., Rix, H.-W., & Hogg, D. W. 2012, *ApJ*, 751, 131.
- Bressan, A., Marigo, P., Girardi, L., et al. 2012, *MNRAS*, 427, 127.
- Brogaard, K., Jessen-Hansen, J., Handberg, R., et al. 2016, *Astron. Nachr.*, 337, 793.
- Brogaard, K., VandenBerg, D. A., Bruntt, H., et al. 2012, *A&A*, 543, A106.
- Brook, C. B., Kawata, D., Gibson, B. K., & Freeman, K. C. 2004, *ApJ*, 612, 894.
- Cacciari, C., Pancino, E., & Bellazzini, M. 2016, *AN*, 337, 899.
- Campante, T. L., Lund, M. N., Kuszlewicz, J. S., et al. 2016, *ApJ*, 819, 85.
- Casagrande, L., Silva Aguirre, V., Schlesinger, K. J., et al. 2016, *MNRAS*, 455, 987.
- Casey, A. R., Hawkins, K., Hogg, D. W., et al. 2017, *ApJ*, 840, 59.
- Chaplin, W. J., Kjeldsen, H., Bedding, T. R., et al. 2011, *ApJ*, 732, 54.
- Chaplin, W. J., & Miglio, A. 2013, *ARA&A*, 51, 353.
- Chaplin, W. J., Sanchis-Ojeda, R., Campante, T. L., et al. 2013, *ApJ*, 766, 101.
- Cheng, J. Y., Rockosi, C. M., Morrison, H. L., et al. 2012, *ApJ*, 746, 149.
- Chiappini, C. 2009, in: The Galaxy Disk in Cosmological Context, eds. J. Andersen, B. Nordström, & J. Bland-Hawthorn. IAU Symp., Vol. 254, 191–196.
- Chiappini, C. 2015, in: Asteroseismology and Next Generation Stellar Models — EES2014, eds. E. Michel, C. Charbonnel, & B. Dintrans, EAS Publications Series, Vol. 73, 309–341.
- Chiappini, C., Anders, F., Rodrigues, T. S., et al. 2015, *A&A*, 576, L12.
- Chiappini, C., Matteucci, F., & Gratton, R. 1997, *ApJ*, 477, 765.
- Christensen-Dalsgaard, J. 2016, ArXiv e-prints.

<sup>11</sup><http://www.issibern.ch/teams/asterostep/>

<sup>12</sup><http://www.asterostep.eu/>



- Cirasuolo, M., Afonso, J., Carollo, M., et al. 2014, in: Ground-based and Airborne Instrumentation for Astronomy V, 91470N, Proc. SPIE, Vol. 9147.
- CoRoT Team 2016. In CoRoT Team (Ed.), Foreword, EDP Sciences.
- Corsaro, E., Lee, Y.-N., García, R. A., et al. 2017, *Nat. Astron.*, *1*, 0064.
- Cui, X.-Q., Zhao, Y.-H., Chu, Y.-Q., et al. 2012, *Res. Astron. Astrophys.*, *12*, 1197.
- Dalton, G., Trager, S., Abrams, D. C., et al. 2014, in: Ground-based and Airborne Instrumentation for Astronomy V, 91470L, Proc. SPIE, Vol. 9147.
- Davies, G. R., & Miglio, A. 2016, *AN*, *337*, 774.
- Davies, G. R., Silva Aguirre, V., Bedding, T. R., et al. 2016, *MNRAS*, *456*, 2183.
- de Bruijng, J., Perryman, M., Lindegren, L., et al. 2005, *gAIAJDB*-022.
- de Jong, R. S., Barden, S., Bellido-Tirado, O., et al. 2014, in: Ground-based and Airborne Instrumentation for Astronomy V, 91470M, Proc. SPIE, Vol. 9147.
- De Silva, G. M., Freeman, K. C., Bland-Hawthorn, J., et al. 2015, *MNRAS*, *449*, 2604.
- Deheuvels, S., Doğan, G., Goupil, M. J., et al. 2014, *A&A*, *564*, A27.
- Deheuvels, S., García, R. A., Chaplin, W. J., et al. 2012, *ApJ*, *756*, 19.
- DESI Collaboration, Aghamousa, A., Aguilar, J., et al. 2016a, ArXiv e-prints.
- DESI Collaboration, Aghamousa, A., Aguilar, J., et al. 2016b
- Di Matteo, P., Haywood, M., Combes, F., Semelin, B., & Snaith, O. N. 2013, *A&A*, *553*, A102.
- Di Matteo, P., Haywood, M., Gómez, A., et al. 2014, *A&A*, *567*, A122.
- Eggenberger, P., Montalbán, J., & Miglio, A. 2012, *A&A*, *544*, L4.
- Eisenstein, D. J., Weinberg, D. H., Agol, E., et al. 2011, *AJ*, *142*, 72.
- Freeman, K. 2012, *Astrophysics and Space Science Proceedings*, Vol. 26, 137.
- Freeman, K., & Bland-Hawthorn, J. 2002, *ARA&A*, *40*, 487.
- Fuhrmann, K. 2011, *MNRAS*, *414*, 2893.
- Fuhrmann, K., Chini, R., Kaderhandt, L., & Chen, Z. 2017, *MNRAS*, *464*, 2610.
- Gaia Collaboration, Brown, A. G. A., Vallenari, A., et al. 2016a, *A&A*, *595*, A2.
- Gaia Collaboration, Prusti, T., de Bruijne, J. H. J., et al. 2016b, *A&A*, *595*, A1.
- García, R. A., Mathur, S., Salabert, D., et al. 2010, *Science*, *329*, 1032.
- Gibson, B. K., Courty, S., Sánchez-Blázquez, P., et al. 2009, in: *The Galaxy Disk in Cosmological Context*, eds. J. Andersen, B. Nordström, & J. Bland-Hawthorn, IAU Symp. Vol. 254, 445–452.
- Gilmore, G., Randich, S., Asplund, M., et al. 2012, *The Messenger*, *147*, 25.
- Girardi, L., Barbieri, M., Groenewegen, M. A. T., et al. 2012, *Astrophysics and Space Science Proceedings*, *26*, 165.
- Girardi, L., Groenewegen, M. A. T., Hatziminaoglou, E., & da Costa, L. 2005, *A&A*, *436*, 895.
- Gizon, L., Ballot, J., Michel, E., et al. 2013, *PNAS*, *110*, 13267.
- Górski, K. M., Hivon, E., Banday, A. J., et al. 2005, *ApJ*, *622*, 759.
- Grand, R. J. J., Springel, V., Kawata, D., et al. 2016, *MNRAS*, *460*, L94.
- Guedes, J., Mayer, L., Carollo, M., & Madau, P. 2013, *ApJ*, *772*, 36.
- Gustafsson, B., Edvardsson, B., Eriksson, K., et al. 2008, *A&A*, *486*, 951.
- Handberg, R., Brogaard, K., & Miglio, A. 2017, ArXiv e-prints.
- Hawkins, K., Masseron, T., Jofré, P., et al. 2016, *A&A*, *594*, A43.
- Hayden, M. R., Bovy, J., Holtzman, J. A., et al. 2015, *ApJ*, *808*, 132.
- Hayden, M. R., Holtzman, J. A., Bovy, J., et al. 2014, *AJ*, *147*, 116.
- Haywood, M., Di Matteo, P., Lehnert, M. D., Katz, D., & Gómez, A. 2013, *A&A*, *560*, A109.
- Hekker, S., & Christensen-Dalsgaard, J. 2016, ArXiv e-prints.
- Hekker, S., Elsworth, Y., Mosser, B., et al. 2012, *A&A*, *544*, A90.
- Holmberg, J., Nordström, B., & Andersen, J. 2007, *A&A*, *475*, 519.
- Howell, S. B., Sobeck, C., Haas, M., et al. 2014, *PASP*, *126*, 398.
- Huber, D., Bedding, T. R., Stello, D., et al. 2010, *ApJ*, *723*, 1607.
- Huber, D., Carter, J. A., Barbieri, M., et al. 2013, *Science*, *342*, 331.
- Huber, D., Ireland, M. J., Bedding, T. R., et al. 2012, *ApJ*, *760*, 32.
- Huber, D., Zinn, J., Bojsen-Hansen, M., et al. 2017, ArXiv e-prints.
- Jacobson, H. R., Friel, E. D., Jilková, L., et al. 2016, *A&A*, *591*, A37.
- Jofré, P., Jorissen, A., Van Eck, S., et al. 2016, *A&A*, *595*, A60.
- Jones, B. J. T., & Wyse, R. F. G. 1983, *A&A*, *120*, 165.
- Jordi, C., Gebran, M., Carrasco, J. M., et al. 2010, *A&A*, *523*, A48.
- Kawata, D., & Chiappini, C. 2016, *AN*, *337*, 976.
- Kippenhahn, R., Weigert, A., & Weiss, A. 2012, *Stellar Structure and Evolution*, Springer-Verlag Berlin, Heidelberg.
- Kjeldsen, H., & Bedding, T. R. 1995, *A&A*, *293*, 87.
- Kubryk, M., Prantzos, N., & Athanassoula, E. 2015, *A&A*, *580*, A126.
- Kunder, A., Kordopatis, G., Steinmetz, M., et al. 2017, *AJ*, *153*, 75.
- Lagarde, N., Miglio, A., Eggenberger, P., et al. 2015, *A&A*, *580*, A141.
- Lagarde, N., Robin, A. C., Reylé, C., & Nasello, G. 2017, *A&A*, *601*, A27.
- Lebreton, Y., & Goupil, M. J. 2014, *A&A*, *569*, A21.
- Lillo-Box, J., Barrado, D., Moya, A., et al. 2014, *A&A*, *562*, A109.
- Majewski, S. R., APOGEE Team, & APOGEE-2 Team 2016, *AN*, *337*, 863.
- Majewski, S. R., Schiavon, R. P., Frinchaboy, P. M., et al. 2015, ArXiv e-prints.
- Martell, S. L., Sharma, S., Buder, S., et al. 2017, *MNRAS*, *465*, 3203.
- Martig, M., Fouesneau, M., Rix, H.-W., et al. 2016, *MNRAS*, *456*, 3655.
- Martig, M., Rix, H.-W., Silva Aguirre, V., et al. 2015, *MNRAS*, *451*, 2230.
- Masseron, T., & Gilmore, G. 2015, *MNRAS*, *453*, 1855.
- Masseron, T., & Hawkins, K. 2017, *A&A*, *597*, L3.
- Mathur, S., García, R. A., Huber, D., et al. 2016, *ApJ*, *827*, 50.
- Matteucci, F. (ed.). 2001, *The Chemical Evolution of the Galaxy*, Astrophysics and Space Science Library, Vol. 253.
- Mazumdar, A., Michel, E., Antia, H. M., & Deheuvels, S. 2012, *A&A*, *540*, A31.
- Michalik, D., Lindegren, L., Hobbs, D., & Lammers, U. 2014, *A&A*, *571*, A85.
- Miglio, A., Chaplin, W. J., Brogaard, K., et al. 2016, *MNRAS*, *461*, 760.
- Miglio, A., Chiappini, C., Morel, T., et al. 2013, *MNRAS*, *429*, 423.
- Miglio, A., Montalbán, J., Carrier, F., et al. 2010, *A&A*, *520*, L6.
- Mikolaitis, Š., Hill, V., Recio-Blanco, A., et al. 2014, *A&A*, *572*, A33.
- Minchev, I., Chiappini, C., & Martig, M. 2013, *A&A*, *558*, A9.
- Minchev, I., Chiappini, C., & Martig, M. 2014, *A&A*, *572*, A92.
- Minchev, I., & Famaey, B. 2010, *ApJ*, *722*, 112.
- Minchev, I., Martig, M., Streich, D., et al. 2015, *ApJ*, *804*, L9.
- Minchev, I., Steinmetz, M., Chiappini, C., et al. 2017, *ApJ*, *834*, 27.
- Miville-Deschênes, M.-A., & Lagache, G. 2005, *ApJS*, *157*, 302.
- Molenda-Žakowicz, J., Brogaard, K., Niemczura, E., et al. 2014, *MNRAS*, *445*, 2446.
- Morel, T. 2015, in: *Asteroseismology of Stellar Populations in the Milky Way*, eds. A. Miglio, P. Eggenberger, L. Girardi, & J. Montalbán, *Astrophysics and Space Science Proc.*, Vol. 39, 73.
- Morel, T., Miglio, A., Lagarde, N., et al. 2014, *A&A*, *564*, A119.
- Mosser, B. 2017, in preparation.
- Mosser, B., & Appourchaux, T. 2009, *A&A*, *508*, 877.
- Mosser, B., Goupil, M. J., Belkacem, K., et al. 2012, *A&A*, *548*, A10.
- Naab, T., & Ostriker, J. P. 2016, ArXiv e-prints.
- Nataf, D. M. 2016, *PASA*, *33*, e023.
- Ness, M., Hogg, D. W., Rix, H.-W., et al. 2016, *ApJ*, *823*, 114.
- Noels, A., & Bragaglia, A. 2015, in: *Asteroseismology of Stellar Populations in the Milky Way*, eds. A. Miglio, P. Eggenberger, L. Girardi, & J. Montalbán, *Astrophysics and Space Science Proc.*, Vol. 39, 167.
- Noels, A., Montalbán, J., & Chiappini, C. 2016, *AN*, *337*, 982.
- Noguchi, M. 1998, *Nature*, *392*, 253.
- Pagel, B. E. J. 2009, *Nucleosynthesis and Chemical Evolution of Galaxies*, Cambridge University Press: Cambridge, UK.
- Pancino, E., Lardo, C., Altavilla, G., et al. 2017, *A&A*, *598*, A5.
- Pérez Hernández, F., García, R. A., Corsaro, E., Triana, S. A., & De Ridder, J. 2016, *A&A*, *591*, A99.
- Pinsonneault, M. H., Elsworth, Y., Epstein, C., et al. 2014, *ApJS*, *215*, 19.
- Plez, B. 2012, *Turbospectrum: Code for Spectral Synthesis*, *Astrophysics Source Code Library*.
- Quillen, A. C., & Garnett, D. R. 2001, in: *Galaxy Disks and Disk Galaxies*, eds. J. G. Funes & E. M. Corsini, *Astronomical Society of the Pacific Conf. Ser.*, Vol. 230, 87–88.
- Quillen, A. C., Minchev, I., Bland-Hawthorn, J., & Haywood, M. 2009, *MNRAS*, *397*, 1599.
- Rauer, H., Catala, C., Aerts, C., et al. 2014, *ExA*, *38*, 249.
- Reddy, B. E., Lambert, D. L., & Allende Prieto, C. 2006, *MNRAS*, *367*, 1329.
- Reese, D. R. 2016, *AIMS: Asteroseismic Inference on a Massive Scale*, *Astrophysics Source Code Library*.
- Rendle, B., Miglio, A., & Reese, D. 2017, in preparation.
- Ricker, G. R., Winn, J. N., Vanderspek, R., et al. 2015, *J. Astron. Telesc. Instrum. Syst.*, *1*, 014003.
- Rix, H.-W., & Bovy, J. 2013, *A&ARv*, *21*, 61.
- Robin, A. C., Reylé, C., Fliri, J., et al. 2014, *A&A*, *569*, A13.
- Rodrigues, T. S., Bossini, D., Miglio, A., et al. 2017, *MNRAS*, *467*, 1433.
- Rodrigues, T. S., Girardi, L., Miglio, A., et al. 2014, *MNRAS*, *445*, 2758.
- Rojas-Arriagada, A., Recio-Blanco, A., de Laverny, P., et al. 2016, *A&A*, *586*, A39.
- Salaris, M., Pietrinferni, A., Piersimoni, A. M., & Cassisi, S. 2015, *A&A*, *583*, A87.
- Samadi, R., Belkacem, K., Dupret, M.-A., et al. 2012, *A&A*, *543*, A120.
- Sandquist, E. L., Jessen-Hansen, J., Shetrone, M. D., et al. 2016, *ApJ*, *831*, 11.
- Schlegel, D. J., Finkbeiner, D. P., & Davis, M. 1998, *ApJ*, *500*, 525.
- Sellwood, J. A., & Binney, J. J. 2002, *MNRAS*, *336*, 785.

- Sharma, S., Bland-Hawthorn, J., Johnston, K. V., & Binney, J. 2011, *ApJ*, 730, 3.
- Shen, J., & Li, Z.-Y. 2016, *Galactic Bulges Astrophysics and Space Science Library*; Springer International Publishing: Switzerland. Vol. 418, 233.
- Silva Aguirre, V., Casagrande, L., Basu, S., et al. 2012, *ApJ*, 757, 99.
- Silva Aguirre, V., Davies, G. R., Basu, S., et al. 2015, *MNRAS*, 452, 2127.
- Snaith, O., Haywood, M., Di Matteo, P., et al. 2015, *A&A*, 578, A87.
- Sommer-Larsen, J., Götz, M., & Portinari, L. 2003, *ApJ*, 596, 47.
- Steinmetz, M. 1994, Mueller, E., *A&A*, 281, L97.
- Steinmetz, M., Zwitter, T., Siebert, A., et al. 2006, *AJ*, 132, 1645.
- Stello, D., Huber, D., Sharma, S., et al. 2015, *ApJ*, 809, L3.
- Stello, D., Vanderburg, A., Casagrande, L., et al. 2016, *ApJ*, 832, 133.
- Turon, C., Primas, F., Binney, J., et al. 2008, *The Messenger*, 134, 46.
- Valentini, M., Chiappini, C., Davies, G. R., et al. 2017, *A&A*, 600, A66.
- Valentini, M., Chiappini, C., Miglio, A., et al. 2016, *AN*, 337, 970.
- Vrard, M., Mosser, B., Barban, C., et al. 2015, *A&A*, 579, A84.
- Wang, L., Wang, W., Wu, Y., et al. 2016, *AJ*, 152, 6.
- Wegg, C., Gerhard, O., & Portail, M. 2015, *MNRAS*, 450, 4050.
- Wisnioski, E., Förster Schreiber, N. M., Wuyts, S., et al. 2015, *ApJ*, 799, 209.
- Wuyts, E., Wisnioski, E., Fossati, M., et al. 2016, *ApJ*, 827, 74.
- Yanny, B., Rockosi, C., Newberg, H. J., et al. 2009, *AJ*, 137, 4377.

**How to cite this article:** Miglio A, Chiappini C, Mosser B, et al. PLATO as it is: A legacy mission for Galactic archaeology. *Astron. Nachr. / AN*. 2018;338:644–661. <https://doi.org/10.1002/asna.201713385>